Reply to Comments from Reviewer #1

We appreciate the constructive and thoughtful comments from the reviewers which have helped us improve the manuscript. We have carefully revised our manuscript following the reviewer's comments. A point-to-point response is given below. The reviewers' comments are in black and our replies are in blue.

To reviewer

Comment 1:

Zhou et al., studied Hg evasion from a subtropical forest and a temperate forest, and they found that fluxes showed strong positive relationships with solar radiation and soil temperature, and negative correlations with ambient-air TGM concentration in both subtropical and temperate forests. They highlighted more attention should pay to the legacy Hg stored in terrestrial surface as a more important increasing Hg emission source with the decreasing air TGM concentration recently. Generally, this study demonstrates some interesting observation in forest air-soil flux exchanges, and these new finding can help us to better understand the Hg fluxes. But I have some concerned issues need the authors to further polish this manuscript before accept.

Response: We thank the reviewer's constructive comments on this manuscript. We have addressed all the reviewer's concerned issues below. We hope the revised manuscript can meet the standards for publication in *Atmospheric Chemistry and Physics*.

Comment 2:

Many studies have suggested that solar radiation and soil temperature have strong effects to induce soil Hg evasion from soil. Authors also have stated these earlier studies results. To me, I am not surprised these results. There are significant correlations among temperature and solar radiation. The effects of these environmental factors on Hg0 flux are confounded. However, the synergistic effect from multiple factors leads to hard determine the individual effect of each parameter. Recently, I also read a subtropical forest air-soil Hg0 flux study in China (Yuan, Wei; Wang, Xun; Lin, Che-Jen.; Sommar, Jonas; Lu, Zhiyun; Feng, Xinbin, Process factors driving dynamic exchange of elemental mercury vapor over soil in broadleaf forest ecosystems. Atmos Environ 2019, 219, 117047). They used SEM equations to demonstrate the temperature is the key parameter to shape

1

31 the soil Hg0 evasion. I wonder does temperature play the similar role in this study as Yuan's study,

32 and I also suggest using similar SEM to further demonstrate the effects from atmospheric Hg0, land

33 use, environmental parameters.

34 Response: We appreciate the reviewer's suggestions. We agree that the synergistic effects from

35 multiple factors makes in difficult evaluate the effect of each factor. The SEM approach was applied

36 the observations in this study following the reviewer's suggestion The results of SEM is shown in

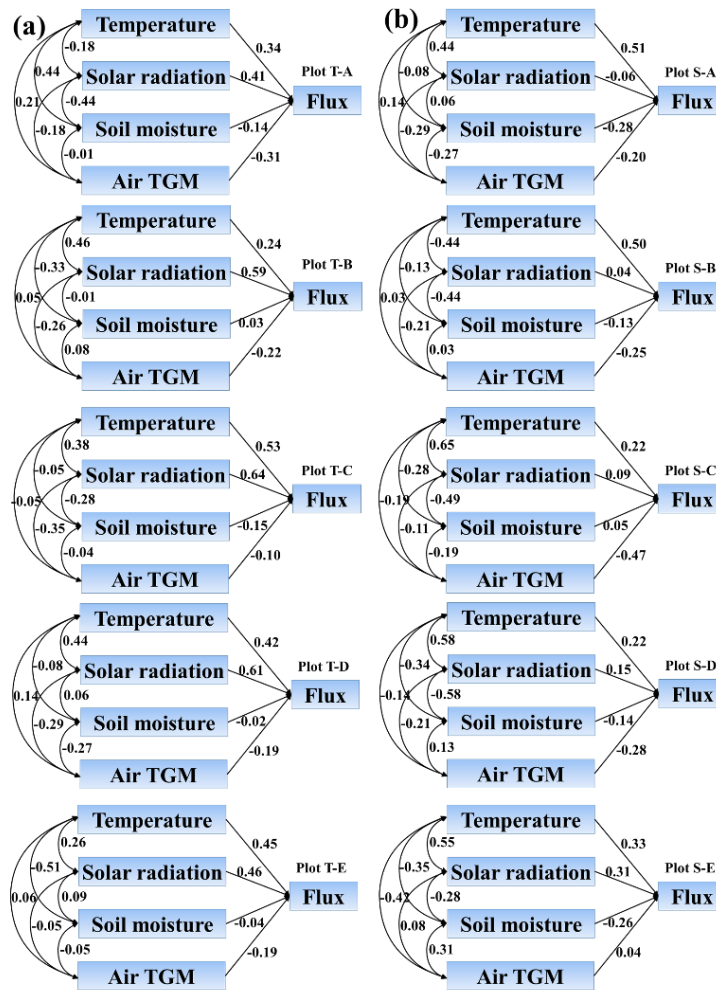37 Fig. 5 and is described in the revised manuscript on lines 239-242, 411-416, 461-463, and 473-475:

39 **Fig. 5.** The interplay of environmental factors on air-soil TGM exchange fluxes determined by

40 structural equation model (SEM) in the temperate (a) and subtropical (b) forests.

41 "Structural equation modeling (SEM) were performed on the collected Hg flux data using Amos

42 software. SEM, developed from a fully conceptual model using χ^2 tests with maximum likelihood

43 estimation, was conducted to infer the interplay of temperature, solar radiation, soil moisture, and

44 air TGM concentrations on measurements of soil-air TGM exchange fluxes."

"To consider synergistic effects from multiple factors, SEM was applied to infer the soil-air TGM exchange processes (Fig. 5). It is clear that temperature was a more dominant factor driving air-soil TGM exchange flux over the four seasons in the subtropical forest plots, while solar radiation was a more dominant factor at the temperate forest due to direct exposure of the forest floor to solar radiation the leaf-off seasons. At the open fields of both forests, temperature and solar radiation had a synergistic effect on soil Hg fluxes."

"Soil-air Hg fluxes also showed significant negative correlations with atmospheric TGM concentrations at the ten plots at both forests ($r^2 = 0.023-0.26$, $p < 0.05$, Fig. 6 and 7), which had a greater effect than soil moisture at both forests, except for plots T-C, S-A and S-E (Fig. 5)."

"SEM inferred that that air TGM concentrations was the second important driver influencing the soil-air TGM exchange in Masson pine (Plot S-B), evergreen broad-leaved and wetland plots at subtropical forest (Fig. 5)."

Comment 3:

There are several forest air-soil Hg fluxes studies in subtropical regions in China, such as Yuan 2019, and Yu et al., 2020 (Subtropical Forests Act as Mercury Sinks but as Net Sources of Gaseous Elemental Mercury in South China, Environ Sci Technol). I suggest authors should compare their results to those studies to support your several hypotheses.

Response: We thank the reviewer for these suggestions. We have added the text comparing our results with Yuan et al. 2019, Yu et al. 2020 and some other studies, these modification are added in the lines 105-113 and 416-420:

"Forest ecosystems not only act as sinks for atmospheric Hg deposition, but can also serve as sources resulting from legacy Hg that has accumulated in surface soil. For example, one study constructed the Hg budget in subtropical forest in southern China showing that the forest is a minor sink for atmospheric Hg but a significant net Hg(0) source (58.5 μg m^{-2} yr^{-1}) (Yu et al., 2020). In contrast, another study also in southern China using budgets of air-foliage and air-soil Hg(0) exchange fluxes, showed that forest is a net sink of Hg(0) (20.1 μg m^{-2} yr^{-1}) (Yuan et al., 2019a; Yuan et al., 2019b). These results indicate that there is considerable uncertainty and variability in the source-sink behavior of Hg in subtropical forests of southern China. Furthermore, no studies have conducted in northern China to characterize the Hg fluxes in the temperate forest."

"A recent study of soil-air TGM fluxes at subtropical evergreen broadleaf forest in South China also suggested that temperature is the most important driver of air-soil TGM exchange (Yuan et al., 2019b). Therefore, we may infer that under the shade of the forest canopy, temperature is the dominant factor causing variation in TGM evasion from forest soil."

Comment 4:

The most interesting results in this study is that air-soil flux varies with the landuse, and distinctly different compensation point for each landuse. However, authors just depicted these results without further explanation and hypothesis.

Response: We have added discussion on the implications of changes in the forest stand landscape and climate on soil mercury dynamics on lines 516-528:

"A recent study using models simulating the dynamics of the subtropical forest landscape under climate change, harvesting, and land-use disturbances in southern China showed that coniferous forest area increased approximately 3.7 times compared to broad-leaved forest area (Wu et al., 2019). In the temperate forest, climatic changes in the northern China are expected to cause coniferous stands to transition to deciduous forests over the next hundred years (Ma et al., 2014). Climate change and land-use disturbance may increase the compensation points in both temperate and subtropical forests, therefore, increasing emissions of legacy Hg from terrestrial soils to the atmosphere. Some studies have emphasized that climate and land use change will potentially enhance deposition of Hg to forested landscapes (Haynes et al., 2017;Richardson and Friedland, 2015;Li et al., 2020); however, our study suggests that legacy Hg in forest soils could be emitted back to atmosphere, offsetting enhanced atmospheric Hg deposition. Better understanding of the response of Hg emissions from forest soils to climate and land use change is an important topic for future research."

Comment 5:

Line 24, "estimates" grammar wrong.

Response: The word has been revised to "estimate"

Comment 6:

105   Line 25, "soil-atmosphere exchange, soil-air gaseous Hg" why repeat twice?

106   Response: The "soil-atmosphere exchange" has been deleted.

107

108   ***Comment 7:***

109   Line 27-28, "showed patterns of both emission and deposition at five study plots, with an area-

110   weighted net emission rate of 3.2 and 0.32âAL'ngâ ˘ AL'm ˘ -2âAL'hr ˘ -1 for the entire subtropical

111   and temperate forests, respectively". This sentence is confused, which forest is a Hg sink or source?

112   Response: We have deleted the sentence and added values to describe the deposition or emission

113   values of the plots in line 28-36:

114   "At the subtropical forest the highest net soil Hg emissions were observed for an open field (24

115        $\pm$ 33 ng m^{-2} hr^{-1}), followed by two coniferous forest plots (2.8 $\pm$ 3.9 and 3.5 $\pm$ 4.2 ng m^{-2} hr^{-1}),

116   broad-leaved forest plot (0.18 $\pm$ 4.3 ng m^{-2} hr^{-1}), and the remaining wetland site showing net

117   deposition (-0.80 ± 5.1 ng m^{-2} hr^{-1}). At the temperate forest, the highest fluxes and net soil Hg

118   emissions were observed for a wetland (3.81 $\pm$ 0.52 ng m^{-2} hr^{-1}) and an open field (1.82 $\pm$ 0.79 ng

119   m^{-2} hr^{-1}), with lesser emission rates in deciduous broad-leaved forest (0.68 $\pm$ 1.01 ng m^{-2} hr^{-1}) and

120   deciduous needle-leaved forest (0.32 $\pm$ 0.96 ng m^{-2} hr^{-1}) plots, and net deposition at an evergreen

121   pine forest (-0.04 ± 0.81 ng m^{-2} h^{-1})."

122

123   ***Comment 8:***

124   Line 29-31 rephrase this sentence because of very hard to understand.

125   Response: The sentence has been rephrased in line 28-32:

126   "At the subtropical forest the highest net soil Hg emissions were observed for an open field (24

127        $\pm$ 33 ng m^{-2} hr^{-1}), followed by two coniferous forest plots (2.8 $\pm$ 3.9 and 3.5 $\pm$ 4.2 ng m^{-2} hr^{-1}),

128   broad-leaved forest plot (0.18 $\pm$ 4.3 ng m^{-2} hr^{-1}), and the remaining wetland site showing net

129   deposition (-0.80 ± 5.1 ng m^{-2} hr^{-1})."

130

131   ***Comment 9:***

132   Line 35 rephrase "at" to "in"

133   Response: The text was changed accordingly in line 37.

134

Comment 10:

Line 51 rephrase this sentence because of unclear

Response: The sentence has been rephrased in line 54-56.

"Hg(0) is relatively inert and has a long atmospheric lifetime of 0.5–1 year, which allows for long range transport (Kamp et al., 2018;Slemr et al., 2018;St Louis et al., 2019)."

Comment 11:

Line 94 I did get your logic flow here when authors stated "serve as sources of previously deposited Hg".

Response: The sentence has been rephrased in line 105-106:

"Forest ecosystems not only act as sinks for atmospheric Hg deposition, but can also serve as sources resulting from legacy Hg that has accumulated in surface soil."

Comment 12:

Line 101, I recently read several subtropical forest studies in China, and authors stated "scarce" is not right.

Response: We have deleted the sentence.

Comment 13:

Line 116. Wrong sentence for "Dongling (MDL)..."

Response: The sentence has been rephrased in line 129-130:

"This study was conducted at TFP in the subtropical zone (106°41.24′E, 29°37.42′N) and at MDL in the temperate zone (115°26′, E40°00' N) in China (Fig. 1)."

Soil-atmosphere exchange flux of total gaseous mercury (TGM) at subtropical and temperate forest catchments

Jun Zhou [a, b, c, f], Zhangwei Wang [a, c, *], Xiaoshan Zhang [a, c], Charles T. Driscoll [d], Che-Jen Lin [e]

a. State Key Laboratory of Urban and Regional Ecology, Research Center for Eco-Environmental Sciences, Chinese Academy of Sciences, Beijing 100085, China.

b. Key Laboratory of Soil Environment and Pollution Remediation, Institute of Soil Science, Chinese Academy of Sciences, Nanjing 210008, China.

c. University of Chinese Academy of Sciences, Beijing 100049, China.

d. Department of Civil and Environmental Engineering, Syracuse University, 151 Link Hall, Syracuse, New York 13244, United States.

e. Center for Advances in Water and Air Quality, Lamar University, Beaumont, Texas 77710, United States.

f. Department of Environmental, Earth and Atmospheric Sciences, University of Massachusetts, Lowell, 01854, USA

* Corresponding author: Zhangwei Wang

E-mail address: wangzhw@rcees.ac.cn (Z. Wang); Phone: +86 10 62849168.

No.18 Shuangqing Road, Beijing 100085, China

First author e-mail: zhoujun@issas.ac.cn (J. Zhou); Phone: +86 25 86881319.

No.73 East Beijing Road, Nanjing 210008, China.

Abstract: Evasion from soil is the largest source of mercury (Hg) to the atmosphere from terrestrial ecosystems. To improve understanding of controls and in estimates of forest soil-atmosphere fluxes of total gaseous Hg (TGM), measurements were made using dynamic flux chambers (DFC) over 130 and 96 days for each of five plots at a subtropical forest and a temperate forest, respectively. At the subtropical forest the highest net soil Hg emissions were observed for an open field (24 ± 33 ng m^{-2} hr^{-1}), followed by two coniferous forest plots (2.8 ± 3.9 and 3.5 ± 4.2 ng m^{-2} hr^{-1}), broad-leaved forest plot (0.18 ± 4.3 ng m^{-2} hr^{-1}), and the remaining wetland site showing net deposition (-0.80 ± 5.1 ng m^{-2} hr^{-1}). At the temperate forest, the highest fluxes and net soil Hg emissions were observed for a wetland (3.81 ± 0.52 ng m^{-2} hr^{-1}) and an open field (1.82 ± 0.79 ng m^{-2} hr^{-1}), with lesser emission rates in deciduous broad-leaved forest (0.68 ± 1.01 ng m^{-2} hr^{-1}) and deciduous needle-leaved forest (0.32 ± 0.96 ng m^{-2} hr^{-1}) plots, and net deposition at an evergreen pine forest (-0.04 ± 0.81 ng m^{-2} h^{-1}). High solar radiation and temperature during summer resulted in the high Hg emissions in the subtropical forest, and the open field and evergreen pine forest at the temperate forest. At the temperate deciduous plots, the highest Hg emission occurred in spring during leaf-off period due to direct solar radiation exposure to soils. Fluxes showed strong positive relationships with solar radiation and soil temperature, and negative correlations with ambient-air TGM concentration in both subtropical and temperate forests, with area-weighted compensation points of 6.82 and 3.42 ng m^{-3}, respectively. The values of the compensation points suggest that the atmospheric TGM concentration can play a critical role in limiting TGM emissions from the forest floor. Climate change and land-use disturbance may increase the compensation points in both temperate and subtropical forests. Future research should focus on the role of legacy soil Hg in reemissions to the atmosphere as decreases in primary emissions drive decreases in TGM concentrations and disturbance of climate change and land use.

Keywords: soil-air flux of total gaseous mercury; dynamic flux chamber; compensation point; climate change; land use

1. Introduction

Mercury (Hg) is a persistent, bio-accumulative, toxic and well-established global contaminant (Obrist et al., 2018). Unlike other trace metals in the atmosphere, the Hg mainly exists as gaseous elemental Hg (Hg(0)), which accounts more than 90% of total gaseous Hg (TGM). Hg(0) is relatively inert and has a long atmospheric lifetime of 0.5–1 year, which allows for long range transport (Kamp et al., 2018;Slemr et al., 2018;St Louis et al., 2019). Global long-range atmospheric transport and deposition is the main pathway of Hg input to remote ecosystems (Lin et al., 2019;Ly Sy Phu et al., 2019;Sun et al., 2019). Soils account for more than 90% of Hg stored in terrestrial ecosystems (Obrist, 2012), with global top soil Hg pools (0–40 cm) estimated at > 300 000 Mg (Hararuk et al., 2013;Zhou et al., 2017a). The large soil Hg pools not only stem from geologic sources, but also from a legacy of historically anthropogenic emissions over the centuries (Obrist et al., 2014;Du et al., 2019).

Although many studies have focused on primary anthropogenic Hg emissions, releases from natural source materials is also an important pathway but with greater uncertainty and variability, including emissions from natural reservoirs (e.g. volcanic activity, geothermal sources, weathering of Hg from soil minerals) and re-emissions of previous deposited Hg. These natural sources can be equal to or two-fold larger than anthropogenic sources (Outridge et al., 2018;Fraser et al., 2018). Recent global Hg models estimate that 3600 Mg yr^{-1} of atmospheric Hg is deposited to terrestrial surfaces, with 1000 Mg yr^{-1} re-emitted back to the atmosphere (Outridge et al., 2018). Moreover, compared to primary anthropogenic emissions of Hg (2500 Mg yr^{-1}), estimates of re-emissions from soil surfaces are highly uncertain (Outridge et al., 2018;Wang et al., 2018). Compiling data from 132 studies, Agnan et al. (2016) found that the Earth's surface (particularly in East Asia) is an increasingly important source of total gaseous Hg (TGM) emissions, with up to half of the global emissions derived from natural sources. They estimated terrestrial TGM emissions of 607 Mg yr^{-1}, but with a large uncertainty range of −513 to 1353 Mg yr^{-1}. Additionally, a recent review suggests that future research should focus on campaigns to understand forest Hg behavior and long-term Hg observations, particularly in Asia (Zhang et al., 2019b).

Forest soils receive Hg inputs from: 1) throughfall that include wet deposition plus the wash off of Hg (II) deposited on foliage surfaces; 2) litterfall that contains foliage and other plant materials that have assimilated atmospheric Hg(0); and 3) direct dry Hg deposition to soil from the atmosphere

9

(Teixeira et al., 2018;Risch et al., 2017;Olson et al., 2018;Cheng et al., 2020). Mercury outputs from forest soils occur from surface or subsurface runoff and air-land surface evasion. Forest soils are highly complex media, with important features that affect soil-air exchange, including soil physio-chemical characteristics (e.g., porosity, oxygen availability, redox potential, organic matter, pH) (Obrist et al., 2010;Carpi et al., 2014). Other factors also influence this process, such as meteorological conditions (e.g., solar radiation, air temperature, precipitation) (Zhou et al., 2015;O'Connor et al., 2019), atmospheric chemistry (ozone, nitrate and hydroxyl radicals) (Peleg et al., 2015;Angot et al., 2016), atmospheric TGM concentrations (Wang et al., 2007) and biological processes (Obrist et al., 2010;Chen et al., 2017). Therefore, to characterize and quantify land-atmosphere exchange of TGM, it is necessary to understand the roles of these factors in mediating this process.

Field studies have shown that elevated anthropogenic Hg emissions in South-East Asia have resulted high atmospheric Hg concentrations an deposition regionally (Kumari et al., 2015;Pan et al., 2010;Zhang et al., 2019b). Forests experience particularly elevated net Hg loads due to enhanced deposition associated with the tree canopy, especially in China (Wang et al., 2016;Zhang et al., 2019a). The annual loading of THg to subtropical forests in China have been shown to be much higher than forest catchments in Europe and North America (Wright et al., 2016;Zhou et al., 2020). High Hg deposition has resulted in elevated soil Hg pools in Chinese subtropical forests (Wang et al., 2018;Wang et al., 2009). In contrast, a recent study showed that the Hg deposition and soil Hg concentrations at a temperate forest in China were similar to those in Europe and North America (Zhou et al., 2020). The forested area in China is 2.2×10^4 km^2, with about 50% and 40% occurring in subtropical and temperate zones, respectively. Therefore, it seems likely that subtropical and temperate forests in China, with contrasting climate, vegetation cover, and atmospheric Hg deposition, may also show different patterns of Hg cycling.

Forest ecosystems not only act as sinks for atmospheric Hg deposition, but can also serve as sources resulting from legacy Hg that has accumulated in surface soil. For example, one study constructed the Hg budget in subtropical forest in southern China showing that the forest is a minor sink for atmospheric Hg but a significant net Hg(0) source (58.5 µg m^{-2} yr^{-1}) (Yu et al., 2020). In contrast, another study also in southern China using budgets of air-foliage and air-soil Hg(0) exchange fluxes, showed that forest is a net sink of Hg(0) (20.1 µg m^{-2} yr^{-1}) (Yuan et al., 2019a;Yuan

269 et al., 2019b). These results indicate that there is considerable uncertainty and variability in the

270 source-sink behavior of Hg in subtropical forests of southern China. Furthermore, no studies have

271 conducted in northern China to characterize the Hg fluxes in the temperate forest.

272   There has been much research characterizing Hg fluxes between the forest floor and the

273 atmosphere from studies worldwide, as reviewed by Zhu et al. (2016) and Agnan et al. (2016). In

274 this paper, we present measurements on atmosphere-land Hg fluxes conducted over 130-days and

275 96-days, respectively, during four seasons for five sites both at a temperate forest catchment at Mt.

276 Dongling (MDL) and a subtropical forest catchment at Tieshanping Forest Park (TFP) in China. The

277 aims of this investigation were to (1) characterize the air-land surface Hg fluxes in different

278 terrestrial ecosystems; (2) conduct detailed field measurements to characterize the uncertainty of

279 land use and climate change in air-surface fluxes of TGM in forest catchments; and (3) to compare

280 estimates of Hg emissions from forest soils at temperate and subtropical zones. We hypothesize that

281 a multi-plot and multi-seasonal study of soil-air fluxes in each forest system will provide new

282 perspectives on the climate change and land use on the soil-air Hg fluxes, and improve

283 understanding and estimates of soil Hg evasion from forest ecosystems.

284

285 **2. Materials and methods**

286 **2.1. Study area**

287   This study was conducted at TFP in the subtropical zone (106°41.24′E, 29°37.42′N) and at

288 MDL in the temperate zone (115°26′, E40°00' N) in China (Fig. 1). The TFP is dominated by a

289 Masson pine (*Pinus massoniana* Lamb.) stand (conifer) with some associated species, such as

290 camphor (*Cinnamom camphora*) and Gugertree (*Schima superba* Gardn), which were planted in

291 1960s following the loss of a natural Masson pine forest. The forest is located about 20 km northeast

292 of Chongqing City, at an altitude from 200 to 550 m. The mean annual precipitation is 1028 mm,

293 with 75% of the rainfall occurring from May to October. The mean annual air temperature is 18.2 °C.

294 The total area of the study forest in the TFP is 1.06×10^3 ha. The soil is typically mountain yellow

295 earth (corresponding to an Acrisol in the FAO) (FAO, 1988), with clay mineralogy dominated by

296 kaolinite (Zhou et al., 2016).

297   Mt. Dongling is near the Beijing Forest Ecosystem Research Station, Chinese Academy of

298 Sciences, which is located 110 km southwest of mega-city Beijing in North China. The elevation is

1300 m asl. The annual average rainfall is 612 mm and mean relative humidity is 66%. The climate of the region is predominantly warm temperate continent monsoon with an annual average temperature of 4.8 °C and precipitation of 611.9 mm. Soil type is mountain brown earth (corresponding to a Eutric cambisol in FAO) (FAO, 1988) (Zhou et al., 2018). The relatively cool climate in the study area has resulted in deep litter and high organic matter concentrations (Fang et al., 2007). The study area is a mature, secondary forest protected since the 1950s following the extensive deforestation. Hg concentrations in environmental media at the site are provided in the Supporting Information (SI, Supporting Text).

2.2. Dynamic flux chamber (DFC) measurement

To reduce the spatial uncertainty in Hg fluxes, different ecosystems were selected for study in a sub-catchment at the subtropical TFP, including a coniferous forest (plots S-A and S-B), a wetland (plot S-C), a broad-leaved (camphor) forest (plot S-D) and an open field with bare soil (plot S-E), and a sub-catchment at the temperate MDL, including a Chinese pine forest (plot T-A), larch forest (plots T-B), wetland (plots T-C), mixed broad-leaved forest (plots T-D) and open field (plots T-E) (Fig. 1). To reduce temporal uncertainty in Hg fluxes, 130-days and 96-days of flux observations were undertaken over four seasons (about one-month of continuous observations for each season, except for one-week during winter at the MDL) (Table S1). The locations of each plot is described in the Table 1 and illustrated in Fig. 1.

Semi-cylindrical quartz glass and open-bottom DFCs (4.71 L) were utilized during the sampling campaign. The area of the DFCs over the soil surface was 20×30 cm, with six inlet holes (1 cm diameter) (Fig. S1). Local fine grained soil was placed outside the chamber to seal any gap between the base of the chamber and the soil. At the outlet of the chamber, an orifice was connected to two exit tubes: one to a regulated suction pump and the other to a gold cartridge for trapping outlet TGM. A sub-stream of air was trapped by a pair of gold quartz cartridges at a flow rate of 0.5 L min^{-1}, which was measured using an integrating volume flow meter. All the gold cartridges were constructed with gold silk (< 0.5 mm diameter). The strands of gold silk were rolled together in a small coil and about 15 coils were used to fill a quartz cartridge with about 2 g of gold. The accuracy of all traps were evaluated (see section 2.4) and non-conforming cartridges were discarded. The chamber flushing flow turnover time (TOT) was 0.47 min and 0.94 min for the subtropical forest

12

329 and temperate forest plots, respectively. The Hg flux was calculated using the following equation:

$$F = (C_0 - C_i) \times Q/A$$

331 where F is the soil Hg flux (ng m^{-2} hr^{-1}); C_o and C_i are the steady state Hg concentrations (ng m^{-3})

332 of the outlet and inlet air streams, respectively, which were calculated by the Hg mass detected in

333 gold cartridges and the corresponding air volume; A is the surface area enclosed by the DFC; Q is

334 the flow rate of ambient air circulated through the DFC (10 L min^{-1} for TFP and 5 L min^{-1} for MDL).

335 High flow rates and short TOTs are appropriate for measuring flux from soils with high Hg

336 concentrations or emissions, while lower flow rates and longer TOT are more appropriate for soils

337 with low Hg concentrations or emissions. Eckley et al. (2010) suggested that the optimal flow was

338 at the beginning of the stable $C_0 - C_i$ (ΔC) period, which was chosen as a compromise between

339 competing criteria aimed at creating conditions inside the DFC similar to the adjacent outside air.

340 Our previous study showed that when ΔC was relative stable, the corresponding flushing flow rate

341 was from 5 to 10 L min^{-1} at the subtropical forest (Zhou et al., 2017a). To avoid suppression of Hg

342 emissions due to the excessive buildup of Hg within the chamber, the flow rate of ambient air

343 circulated through the DFC was 10 L min^{-1} at the subtropical forest. At the temperate forest, the soil

344 Hg concentrations was about 3-4 times lower than those at the subtropical forest, so the lower flow

345 rate of 5 L min^{-1} was used at these plots. The DFC chambers in all plots were moved every week to

346 mitigate against changes in soil moisture due the covering of soil by the chambers. If a precipitation

347 event occurred, the chambers were also moved to new positions during the sampling period

348 (morning or evening) to be representative of soil conditions receiving ambient precipitation.

349 The pair of gold cartridges for each DFC were collected twice a day: every morning (about

350 8:00) and afternoon (about 17:00) representing night (17:00−8:00 of next day) and day (8:00−17:00)

351 emissions, respectively. Twenty gold quartz cartridges were alternated during the sampling program.

352 In addition, diurnal variations of soil-air Hg fluxes were also conducted in each season, with gold

353 cartridges collected every half an hour. A total of four diurnal measurements were conducted over

354 the study in each forest, with diurnal variations were measured one day per season. It has been

355 reported that the DFC measurements can introduce bias under a given design flushing air flow rates

356 and environmental condition (Lin et al., 2010;Zhang et al., 2002). The DFC enclosure imposes a

357 physical constraint that can lead to accumulation in or evasion from the soil surface under

358 measurement. Extensive experiments were conducted at our plot sites to determine the appropriate

13

359 experimental conditions for accurate measurements. We followed recommendations made by

360 Eckley et al. (2010) for our measurements.

361

2.3. Environmental measurements

363   At each sampling plot, soil samples were collected from the DFC footprint (0−5 cm). Soil Hg

364 and soil organic matter (SOM) concentrations were measured using a DMA-80 direct Hg analyzer

365 (Milestone Ltd., Italy) and loss on ignition (LOI) method, respectively, using methods detailed in

366 the SI. Soil percent moisture and temperature were monitored with Time Domain Reflectometry

367 (TDR) Hydra Probe II (SDI−12/RS485) and a Stevens water cable tester (USA). Solar radiation was

368 measured by a weather station (Davis Wireless Vantage VUE 06250 Weather Station, Davis

369 Instruments, Hayward, CA) located in the TFP Forest Station and Beijing Forest Ecosystem

370 Research Station, within about 500 m of each plot.

371

2.4. Quality assurance and quality control (QA/QC)

373   All cartridges were transported to a laboratory at the TFP Forest Station for Hg determination

374 using a cold vapor atomic fluorescence spectroscopy (CVAFS) detector (Brooks Rand III). The limit

375 of detection, based on three times the standard deviation of replicate measurements of the blank was

376 1 pg. Based on the sampled air volume, the detection limits were < 0.10 ng m^{-3}. A calibration curve

377 was developed using Hg saturated air and the calibration curve was required to have a correlation

378 coefficient greater than 0.99 before the samples analysis could proceed. Before and after the

379 measurement of the sampling cartridges in each day, standard Hg saturated air was injected to test

380 the accuracy of the Hg analyzer. If the deviation of the measured Hg mass was higher than 5%, new

381 calibration curve would be developed.

382   A controlled volume of saturated Hg air at a known temperature was injected to measure Hg

383 recovery from the gold cartridges before and after the campaigns in each season. The recoveries of

384 gold cartridges before and after the operation ranged from 98.8 to 103.2% and 96.3 to 102.5%

385 (n=155, average=98.9%), respectively. The collection efficiency of Hg vapor by the gold cartridges

386 was determined by connecting two cartridges in sequence and sampling the ambient air over 24 h

387 in the laboratory. For all cartridges, less than 1% Hg was detected on the second cartridges compared

388 to the first cartridge, indicating that more than > 99% of TGM was absorbed by the gold cartridges

during the field operation. For comparison, Hg fluxes were measured by two chambers side by side

simultaneously. Blanks of the soil TGM flux sampling systems were measured by placing the DFC

on a quartz glass surface in the five plots. The sampling time for blank measurements was same as

soil-air TGM flux measurements, which were collected at 8:00 and 17:00, representing night

(17:00−8:00 of next day) and day (8:00−17:00) emissions, respectively. The averaged blank was

0.13 ± 0.21 ng m^{-2} h^{-1} (n=10), which was subtracted from the soil-air TGM flux for each season.

2.5. Statistical analysis

Structural equation modeling (SEM) were performed on the collected Hg flux data using Amos

software. SEM, developed from a fully conceptual model using $\chi 2$ tests with maximum likelihood

estimation, was conducted to infer the interplay of temperature, solar radiation, soil moisture, and

air TGM concentrations on measurements of soil-air TGM exchange fluxes. Seasonal and annual

fluxes were compared among the ten plots. Separate two-way ANOVAs were used to determine if

differences in Hg fluxes existed among the seasons and sites. All differences in mean values were

significant at the p=0.05 level and all means are reported with ± one standard deviation from the

mean. The correlations between environmental parameters and fluxes were analyzed by Pearson's

Correlation Tests using SPSS software (SPSS Inc. 16.0) and correlation coefficient and p values are

presented and significantly correlated at the level of 0.05.

3. Results and discussion

3.1. Landscape- and forest species-dependence of soil-air Hg fluxes at the forest catchment scale

The soil TGM flux measurements for the five plots were calculated for the day and night and

reported as mean daily fluxes with standard deviations (SD) at the subtropical (Fig. 2a) and

temperate forests (Fig. 2b). Over the course of the campaigns, net TGM emission was observed at

the open field (24 ± 33 ng m^{-2} hr^{-1}), coniferous forest (upper elevation 2.8 ± 3.9 ng m^{-2} hr^{-1}, mid

elevation 3.5 ± 4.2 ng m^{-2} hr^{-1}) and the broad-leaved forest (0.18 ± 4.3 ng m^{-2} hr^{-1}), while net

deposition was evident at the wetland (-0.80 ± 5.1 ng m^{-2} hr^{-1}), respectively, at the subtropical

forest. At the temperate forest, net TGM emission was observed at the wetland (3.81 ± 0.52 ng m^{-2}

hr^{-1}), open field (1.82 ± 0.79 ng m^{-2} hr^{-1}), mixed broad-leaved forest (0.68 ± 1.01 ng m^{-2} hr^{-1}),

419 larch forest (0.32 ± 0.96 ng m^{-2} hr^{-1}), while net deposition was evident at the Chinese pine forest

420 (-0.04 ± 0.81 ng m^{-2} h^{-1}), respectively. The fluxes at the temperate forest were 10-times lower than

421 values at the subtropical forest due to different environmental factors, such as lower temperature,

422 solar radiation and soil Hg concentrations (see section 3.3).

423   These patterns suggest that soil-air Hg fluxes at catchment scale vary by soil properties (e.g.,

424 soil Hg concentration, moisture, SOM) and forest species composition. High variability, as

425 evidenced by high SD and coefficient of variation (SD/mean, range of 14−2374%), was evident in

426 daily Hg fluxes largely driven by meteorological variation. The fluxes at the subtropical forest

427 plots of this study were much lower than those reported for other subtropical evergreen forests in

428 China such as Mt. Gongga ($0.5–9.3$ ng m^{-2} hr^{-1}) (Fu et al., 2008), Mt. Jinyun (14.2 ng m^{-2} hr^{-1})

429 (Ma et al., 2013) and Mt. Simian (11.23 ng m^{-2} hr^{-1}) (Ma et al., 2018), all of which were generally

430 conducted during sunny days. Our flux measurements at temperate forest were slightly lower or

431 comparable to those in North American deciduous forests, ranging from -0.73 to 2.7 ng m^{-2} hr^{-1}

432 (Choi and Holsen, 2009b;Hartman et al., 2009;Carpi et al., 2014;Ma et al., 2018). These results

433 demonstrated that measurements over several days may exhibit considerable temporal variability

434 and long-term study should be undertaken to reduce the uncertainty in temporal patterns of soil Hg

435 emissions.

436   The mean TGM fluxes in the open fields were about 10 and 6 times higher than those under

437 the forest canopy at the subtropical and temperate forests, respectively ($p < 0.001$). Our results are

438 consistent with Ma et al. (2013) and Xin and Gustin (2007), showing large Hg evasion following

439 forest conversion to bare soils due to direct exposure to sunlight, as fluxes were enhanced by

440 increases in solar radiation and temperature. Due to frequent heavy rains at the subtropical forest

441 catchment, a large amount of surface runoff impacted the wetland (plot S-C). Elevated runoff may

442 have decreased Hg (96 ± 43 ng g^{-1}) and SOM in surface soils due to erosion (Table 1). This site had

443 the lowest TGM fluxes of the plots studied at the subtropical forest (overall net sink). In addition,

444 soils in the wetland plot were mostly saturated throughout the year, limiting Hg fluxes and likely

445 contributing to the sink behavior. In contrast, the mean annual rainfall was 40% lower at the

446 temperate forest and the wetland was located at relatively lower terrain. Litter from surrounding

447 higher terrain forest accumulated in the low lying wetland. The cool and dry climate also contributed

448 to high organic matter and low bulk density (Fang et al., 2007). Higher SOM likely facilitated

16

binding of trace metals, leading to high soil Hg concentrations (117 ng g^{-1}) at the temperate wetland. These conditions were conducive to biological activity, promoting the mineralization of SOM and the release of volatile Hg(0) from soil (Choi and Holsen, 2009b;Osterwalder et al., 2019). The wetland had the highest TGM fluxes of the plots studied at the temperate forest (overall net source). Previous studies have suggested that soil water is able to mobilize Hg from binding sites on soil (Gustin, 2003;Kocman and Horvat, 2010) and high soil water decreases soil redox potential (Zarate-Valdez et al., 2006), both of which can facilitate the conversion of Hg(II) to Hg(0). Additionally, the climate is relatively dry in north China, especially in spring. The high solar radiation and relatively high air temperature not only enhance the reduction of Hg(II) to Hg(0), but also increase water evaporation compared to other study sites. Enhanced water evaporation at higher temperature, facilitates Hg emissions from soils (Gustin and Stamenkovic, 2005;Lin et al., 2010). Additionally, given that Hg conversion to Hg(0) in soil profiles occurs mainly via biotic processes, maximum aerobic microbial activity has been delineated at soil water content equivalent to 60% of a soil's water holding capacity (Breuer et al., 2002;Kiese and Butterbach-Bahl, 2002). Appropriate soil moisture in the wetland would likely enhance the microbial reduction of Hg(II) to Hg(0). Therefore, the highest Hg flux was observed in the temperate wetland, especially in spring. The main reasons for the significant differences between the soil Hg fluxes at the two wetland sites is likely that the saturated soil at the subtropical forest inhibited Hg(0) evasion (Gustin and Stamenkovic, 2005) (see section 3.3).

At the subtropical forest, litterfall in the broad-leaved (camphor) plot (plot S-D) was twice as high as that of the coniferous (pine) plot (plots S-A and S-B) (Zhou et al., 2018), likely resulting in greater shielding of sunlight to the surface soil and limiting soil Hg evasion. Increases in light transmission through the canopy increase both solar radiation and soil temperature, which can enhance photochemical reduction of Hg(II) at the soil surface and Hg(0) evasion. In the mid-slope of the pine stand (plot S-B), soil Hg concentration was elevated compared to the upslope plot (Table 1), with corresponding with higher soil Hg fluxes. At the temperate forest, the lowest Hg flux and overall deposition was observed at the evergreen forest of Chinese pine, where the canopy cover likely limited Hg flux by decreasing solar radiation to soil and warming. Similar at the subtropical forest, the needle biomass in the larch plot was about 2.5 times greater as that in the mixed broad-leaved plot (plot T-D) at the temperate forest, resulting in shielding the sunlight to the surface soil

479   and limiting soil Hg evasion at larch plot.

480   The forest canopy not only influences the soil Hg concentration by mediating atmospheric Hg

481   deposition (Zhou et al., 2018;Zhou et al., 2017a), but also alters soil physio-chemical properties (e.g.

482   SOM, pH, porosity) (Mo et al., 2011) and microbial communities (Nagati et al., 2020), which affect

483   soil-air exchange. For example, the annual litterfall Hg deposition flux at the broad-leaved plot (91

484    $\mu g\ m^{-2}\ yr^{-1}$) at the subtropical forest was approximately two times greater than the coniferous plot

485   (41 $\mu g\ m^{-2}\ yr^{-1}$) (Zhou et al., 2018). Conversely, the SOM and soil Hg concentrations in the broad-

486   leaved forest were lower than the coniferous forest. Moreover, litter decomposition rate was lower,

487   but the Hg mass accumulation in the litter was much higher in the coniferous forest compared to the

488   broad-leaved forest due to higher throughfall Hg deposition at the coniferous plot (Zhou et al., 2018),

489   which resulted in a seemingly inconsistent pattern between litterfall mass and SOM, as well as

490   litterfall Hg deposition and soil Hg concentrations. At the temperate forest, the higher litterfall Hg

491   deposition and lower litter decomposition in the larch plot compared to the broad-leaved plot (Zhou

492   et al., 2017a), resulted in significant higher SOM and soil Hg concentrations (Table 1). Tree species

493   can change the physicochemical properties of soil (e.g. SOM, soil Hg concentrations) and influence

494   soil-air exchange. These biological factors likely contribute to the much lower TGM evasion in the

495   broad-leaved plot than the coniferous plot at the subtropical forest, but much higher TGM evasion

496   in the broad-leaved plot than the deciduous needle (larch) plot at the temperate forest (Fig. 2).

497   Most studies measure soil TGM fluxes at only one location or at a single forest stand to

498   characterize the whole ecosystem. Our observations clearly show that soil-air Hg fluxes vary

499   substantially across different plots (Fig. 2), indicating that forest type/cover and landscape position

500   significantly affect the TGM fluxes and therefore the spatial variability in soil Hg fluxes among

501   different sub-plots must be considered. Based on the areal distribution of each plot type in the study

502   sub-catchments of the subtropical forest (coniferous upland and mid-slope, broad-leaved, wetland,

503   open) (4.6 ha) and the temperate forest (Chinese pine, larch, wetland, mixed broad-leaved and

504   open) (5.0 ha) (Table S1), the area-weighted TGM flux was 3.2 and 0.32 ng m^{-2} hr^{-1} for the entire

505   subtropical and temperate catchments, respectively. The area-weighted TGM fluxes were 14%

506   higher than plot S-A and 16% lower than plot S-B of the Masson pine stand at the subtropical

507   forest, and were 907% higher than Chinese pine plot and 53% lower than mixed broad-leaved plot

508   at the temperate forest, respectively. The observations at several plots with diverse forest cover in

509   this study should reduce the overall uncertainty associated with soil-air fluxes of TGM in the

510   overall forest catchment.

511

512   **3.2. Seasonal variations of soil-air Hg fluxes at the forest catchment scale**

513   Soil TGM fluxes not only exhibited clear seasonal variations at all the plots, but also were

514   responsive to phenological and meteorological patterns. At the subtropical forest, soil Hg fluxes

515   were generally highest in the summer (Fig. 2a), which showed net emissions at all the five plots,

516   followed by spring and autumn, with the lowest values during winter, which exhibited net deposition

517   at all plots with the exception of plot S-B. The observed seasonal variation was dependent on

518   sunlight (Fig. 3), because solar radiation drives photochemical reduction of Hg(II) (note the

519   correlation between the TGM fluxes and solar radiation, Fig. S2). Additionally, greater solar

520   radiation increases temperature, which promotes the production of soil Hg gas by biological and

521   abiotic processes. At the temperate forest, the Hg fluxes were the highest in the deciduous forest

522   plot (wetland, mixed broad-leaved forest and larch forest) in spring before leaf-out when solar

523   radiation could directly reach the forest floor (Fig. S3). In the open field and evergreen forest

524   (Chinese pine forest) plots, the Hg fluxes were highest in summer with the highest solar radiation

525   and temperature (Fig. 4 and Fig. S3). The lowest Hg fluxes were measured in the winter at all plots

526   when the soil was covered with snow, with net Hg emission observed at the open field and net

527   deposition observed at the other four sites (Fig. 2b).

528   We also observed strong variation in TGM evasion under different weather conditions. Rain

529   events decreased TGM fluxes at all plots in both forests (Fig. S4), as the rainwater decreased soil

530   pore space leading to decreases in evasion from soil. Furthermore, the solar radiation and

531   temperature during rainy days was much lower than those for sunny days for a given season (Fig. 3

532   and Fig. 4). Manca et al. (2013) studied snow-air Hg exchange at Ny-Ålesund, showing on average

533   a small net deposition -0.24 ng m^{-2} hr^{-1}. Likewise, overall deposition between -0.6 and -23.8 ng m^{-}

534   ^{2} hr^{-1} were observed at snow-covered agricultural areas at Northeastern China (Wang et al.,

535   2013;Zhang et al., 2013). However, some studies of snowpack have shown net Hg deposition at

536   nighttime and net emissions during daytime due to high solar radiation (Maxwell et al.,

537   2013;Spolaor et al., 2019). Empirical models suggest that most of the Hg(0) deposited to snow was

538   re-emitted back to the atmosphere (Durnford and Dastoor, 2011). During the campaigns in winter,

the solar radiation was relatively lower, which may be why net deposition occurred (Fig. 4). Additionally, refrozen ice/snow layers are characterized by elevated Hg concentrations and the deposited Hg from atmosphere could be potentially released to meltwater (Zhang et al., 2012;Perez-Rodriguez et al., 2019), which is consistent with our results that atmospheric Hg deposition could release to meltwater during snow melt. Our observations through the annual climatic cycle reduce uncertainty and bias of temporal patterns of soil-air Hg fluxes. Moreover, multi-plot observations reduce the uncertainty and bias associated with spatial variation. Together these more detailed measurements improved estimates of overall ecosystem soil Hg evasion, and confirm our hypothesis.

3.3. Correlations between environmental factors and fluxes

To investigate the correlation between soil-atmosphere fluxes and environmental factors, data over the four seasons were used. These data offer a long continuous time series for the five measurement plots in each forest (Fig. 3 and 4). According to a global database, atmospheric fluxes at Hg-enriched sites are positively correlated with substrate Hg concentrations, but this relationship is not observed at sites with lower background concentrations of soil Hg (Agnan et al., 2016). Our soil Hg fluxes were strongly correlated with soil Hg concentrations at vegetated sites (forests and wetland) at the subtropical forest (Fig. S5), but not at the temperate forest.

Photo-reduction is a major driver of TGM evasion from the Earth's surface (Howard and Edwards, 2018;Kuss et al., 2018;Gao et al., 2020). This process is due to photochemically mediated reduction that converts soil water Hg(II) to volatile Hg(0) and enhances the Hg(0) pool in soil pores (Xin and Gustin, 2007;Choi and Holsen, 2009a). Therefore, the elevated soil pore Hg(0) concentrations increased the potential for TGM diffusion from soil to the atmosphere, which drives an increase of Hg emissions from soil. At all the study sites no matter the daily average fluxes (Fig. 3 and 4), daytime fluxes (Fig. S2 and S3) were all significantly correlated with solar radiation, and the solar radiation also increased daytime fluxes compare to nighttime values (Fig. S6). In the evergreen plots of the subtropical (plots S-A, S-B, S-D) and temperate (plot T-A) forests, Hg fluxes were the most highly dependent on soil temperature compared to the solar radiation during the four seasons, likely due to evergreen canopy limiting solar radiation to the forest floor. With the consistent shade of the coniferous forest canopy, the Hg flux was highly dependent on soil surface temperature rather than solar radiation to the forest floor.

Mercury fluxes in wetlands in both forests (plots S-C and T-C) were less strongly correlated with soil temperature compared to the other plots in both forests (Fig. S7 and S8). Generally, temperature is an important factor that promotes TGM evasion after its formation from Hg(II) more by biotic than abiotic processes in soils (Pannu et al., 2014). The Hg(0) in soil pore gas mainly results from biotic production. For example, soil sterilization can decrease Hg converted to Hg(0) by ~50% ; additionally, 1% of the soil Hg is converted to Hg(0) via abiotic processes, compared to 6.8% by biotic processes at 283 K, and the fraction of Hg reduction by biotic processes increases with temperature increases (Pannu et al., 2014). At the subtropical forest, the wetland soil was largely saturated. This condition likely limited soil pore release of TGM to the atmosphere, resulting in a weaker correlation between soil temperature and Hg fluxes. Furthermore, the Hg exchange fluxes were more dependent on solar radiation and less dependent on temperature during the leaf-off period at the temperate deciduous plots; therefore, the Hg fluxes were more solar radiation-driven in the deciduous forests, especially in the wetland (Fig. S3 and S7).

During the campaign, significant negative correlations were evident between soil moisture and soil-air fluxes of TGM at the five plots at the subtropical forest ($r^2 = 0.03−0.39$, $p < 0.05$ for all, Fig. S9), but there was no significant correlations with soil moisture for the temperate forest (Fig. S10). Generally there is an optimum soil moisture condition that maximizes soil TGM flux (Gustin and Stamenkovic, 2005;Lin et al., 2010;Obrist et al., 2014;Osterwalder et al., 2018;Johnson et al., 2003), which ranges from 60% to 80% of the water holding capacity of a soil (Pannu et al., 2014). A laboratory experiment using undisturbed soil collected from the our subtropical study area showed

21

that increasing soil moisture from 2% to 20% increased the TGM flux 80% at 24 °C (Wang et al., 2014). A second field experiment was conducted to study the effects of higher soil moisture on TGM flux at the subtropical forest, showing that increasing soil moisture gradually decreased the soil Hg emissions over the range of 31−39% (Zhou et al., 2017b). Combining the results of these experiments, the soil Hg fluxes at the subtropical forest catchment appear to increase from low values of soil moisture reaching an optimum in the range of 20-30% and then decreasing with increasing soil moisture above these values. In the current study, we observed following an extended dry period with an extended wet period enhanced the Hg fluxes in both forests; however, individual rainfall events did not enhance or decrease the Hg fluxes due to short-term increases in soil moisture and lower solar radiation associated with those events (Fig. 3 and 4). Additionally, Lin et al. (2010) observed the synergistic effects (20–30 % of additional flux enhancement) between air temperature (15 and 30 °C) and soil moisture (2.5 and 27.5 %). Perennially humid weather results in relatively high soil moisture at the subtropical forest (largely > 25% during the campaigns). Considering the relatively high bulk density and low porosity of soil at the subtropical forest (Sørbotten, 2011), soil moisture likely exceeded the optimum range for TGM evasion during the campaigns resulting in significantly negative correlations (Fig. S9). In contrast, lower bulk density and higher soil porosity would result in higher optimum range of soil moisture at the temperate forest. Moreover, the temperate forest had a large range of soil moisture (2 to 60%) in the five plots which combined with the synergistic effects of soil moisture with temperature (Lin et al., 2010), resulted in a condition where moisture was not a main driver of TGM evasion.

Soil-air Hg fluxes also showed significant negative correlations with atmospheric TGM concentrations at the ten plots at both forests ($r^2 = 0.023−0.26$, $p < 0.05$, Fig. 6 and 7), which had a greater effect than soil moisture at both forests, except for plots T-C, S-A and S-E (Fig. 5). According to the two-resistance exchange interface model, the exchange fluxes of Hg are controlled by the gradient of TGM concentrations at both interfaces (Zhang et al., 2002). As a result elevated atmospheric TGM concentrations should decrease the diffusion of soil pore TGM to the atmosphere. In a companion study, the soil pore TGM concentrations were measured at all the plots at the subtropical and temperate forests, except the wetlands (Zhou et al., in review). These results showed that gradient of TGM concentrations between the surface air and pore air at 3 cm were significantly correlated with the soil-air TGM fluxes at all the plots (Fig. S11 and S12). These results are

629 consistent with an experiment conducted at this subtropical forest, where artificially increasing

630 ambient-air TGM concentrations significantly inhibited soil Hg volatilization (Zhou et al., 2017b).

631 SEM inferred that that air TGM concentrations was the second important driver influencing the soil-

632 air TGM exchange in Masson pine (Plot S-B), evergreen broad-leaved and wetland plots at

633 subtropical forest (Fig. 5).

634   Xin and Gustin (2007) and Gustin et al. (2006) defined an associated concept of the

635 compensation point for soils, which is the atmospheric Hg concentration at which the net Hg flux

636 between the soil and the atmosphere was zero. If the atmospheric TGM concentration is above

637 compensation point, atmospheric deposition occurs; if the concentration is below the compensation

638 point soil emission occurs. A strong linear relationships are shown in Figs. 5 and 6 ($p < 0.01$),

639 resulting in compensation points of 2.47, 2.97, 6.00, 3.33 and 3.50 ng m^{-3} for Chinese pine, larch,

640 wetland, mixed broad-leaved forests and open field at the temperate forest with area-weighted

641 compensation point of 3.42 ng m^{-3}. The compensation points were much higher at the subtropical

642 forest, with values of 6.50, 7.71, 3.92, 3.83 and 12.91 ng m^{-3} for Masson pine upland and mid-slope,

643 wetland, broad-leaved and open field at the subtropical forest with area-weighted compensation

644 point of 6.82 ng m^{-3}. Another study of subtropical coniferous forest showed similar compensation

645 point (7.75 ng m^{-3}) as those in the Masson pine forests of our study (Luo, 2015).

646   Diurnal variation in soil-air TGM fluxes were measured in plot S-A at the subtropical forest

647 (Fig. 8) and in plot T-D at the temperate forest (Fig. 9). Soil TGM fluxes were well correlated with

648 soil and air temperature ($p < 0.01$ for all) and were highly dependent on solar radiation in spring,

649 summer and autumn ($p < 0.01$ for all) but not in winter ($p > 0.05$), which are similar to seasonal

650 patterns from other studies (Howard and Edwards, 2018;Osterwalder et al., 2018;Johnson et al.,

651 2003). Solar radiation has been shown to promote photochemical reduction of soil-bound Hg and

652 enrich Hg(0) in soil pore gas. This reaction is kinetically enhanced at higher temperatures (Eckley

653 et al., 2015;Lin et al., 2010;Zhang et al., 2001). Compared to the other three seasons, the relatively

654 low soil temperature (5.95 °C at the subtropical forest and –5.66 °C at the temperate forest) may

655 have limited the relationship between soil TGM flux and solar radiation during the winter season.

656

657 **4. Conclusions and study implications**

658   Prior to undertaking these measurements of Hg air-surface exchange flux, no direct

measurement of Hg exchange flux were available for background landscapes in North China. Our detailed direct observations have important implications for the role of forests in global and regional Hg cycles. Through multi-plot measurements over 130 and 96 days at the subtropical and temperate forests in China, we were able to reduce the uncertainty of soil-atmosphere TGM fluxes at the catchment scale and improve understanding of how landscape attributes contribute to variability in soil Hg evasion. It is inferred that forest soils acts as net TGM sources to the atmosphere. Strong correlations were evident between the soil Hg flux and environmental variables in some plots, such as solar radiation, temperature, soil moisture and air TGM concentrations.

The compensation points were determined for background forest soils from full-scale field data showing area-weighted values of 6.82 and 3.42 ng m^{-3} for the entire subtropical and temperate catchments, respectively. The values of compensation indicate that the atmospheric TGM concentration can play a critical role in limiting TGM fluxes between forest floor and atmosphere. Future studies need to focus on forest soils as an important increasing source of Hg to the atmosphere, because of recent declines in anthropogenic Hg emissions and TGM concentrations (Liu et al., 2019). Moreover TGM re-emissions are partially derived from legacy Hg stored in surface soils. A recent study using models simulating the dynamics of the subtropical forest landscape under climate change, harvesting, and land-use disturbances in southern China showed that coniferous forest area increased approximately 3.7 times compared to broad-leaved forest area (Wu et al., 2019). In the temperate forest, climatic changes in the northern China are expected to cause coniferous stands to transition to deciduous forests over the next hundred years (Ma et al., 2014). Climate change and land-use disturbance may increase the compensation points in both temperate and subtropical forests, therefore, increasing emissions of legacy Hg from terrestrial soils to the atmosphere. Some studies have emphasized that climate and land use change will potentially enhance deposition of Hg to forested landscapes (Haynes et al., 2017;Richardson and Friedland, 2015;Li et al., 2020); however, our study suggests that legacy Hg in forest soils could be emitted back to atmosphere, offsetting enhanced atmospheric Hg deposition. Better understanding of the response of Hg emissions from forest soils to climate and land use change is an important topic for future research.

Data availability. The data will be available upon request to the corresponding author.

701

References:

Agnan, Y., Le, D. T., Moore, C., Edwards, G., and Obrist, D.: New constraints on terrestrial surface-atmosphere fluxes of gaseous elemental mercury using a global database, Environmental Science & Technology, 50, 507−524, 10.1021/acs.est.5b04013, 2016.

Angot, H., Dastoor, A., De Simone, F., Gardfeldt, K., Gencarelli, C. N., Hedgecock, I. M., Langer, S., Magand, O., Mastromonaco, M. N., Nordstrom, C., Pfaffhuber, K. A., Pirrone, N., Ryjkov, A., Selin, N. E., Skov, H., Song, S., Sprovieri, F., Steffen, A., Toyota, K., Travnikov, O., Yang, X., and Dommergue, A.: Chemical cycling and deposition of atmospheric mercury in polar regions: review of recent measurements and comparison with models, Atmospheric Chemistry and Physics, 16, 10735-10763, 10.5194/acp-16-10735-2016, 2016.

Breuer, L., Kiese, R., and Butterbachbahl, K.: Temperature and moisture effects on nitrification rates in tropical rain-forest soils, Soil Science Society of America Journal, 66, 399-402, 2002.

Carpi, A., Fostier, A. H., Orta, O. R., dos Santos, J. C., and Gittings, M.: Gaseous mercury emissions from soil following forest loss and land use changes: Field experiments in the United States and Brazil, Atmospheric Environment, 96, 423-429, 10.1016/j.atmosenv.2014.08.004, 2014.

Chen, Y., Yin, Y., Shi, J., Liu, G., Hu, L., Liu, J., Cai, Y., and Jiang, G.: Analytical methods, formation, and dissolution of cinnabar and its impact on environmental cycle of mercury, Critical Reviews in Environmental Science and Technology, 47, 2415-2447, 10.1080/10643389.2018.1429764, 2017.

Cheng, Z., Tang, Y., Li, E., Wu, Q., Wang, L., Liu, K., Wang, S., Huang, Y., and Duan, L.: Mercury accumulation in soil from atmospheric deposition in temperate steppe of Inner Mongolia, China, Environmental Pollution, 258, 10.1016/j.envpol.2019.113692, 2020.

Choi, H.-D., and Holsen, T. M.: Gaseous mercury emissions from unsterilized and sterilized soils: The effect of temperature and UV radiation, Environmental Pollution, 157, 1673-1678, 10.1016/j.envpol.2008.12.014, 2009a.

Choi, H. D., and Holsen, T. M.: Gaseous mercury fluxes from the forest floor of the Adirondacks,

727   Environmental Pollution, 157, 592-600, 2009b.

728 Du, B., Zhou, J., Zhou, L., Fan, X., and Zhou, J.: Mercury distribution in the foliage and soil profiles of
729   a subtropical forest: Process for mercury retention in soils, Journal of Geochemical Exploration, 205,
730   10.1016/j.gexplo.2019.106337, 2019.

731 Durnford, D., and Dastoor, A.: The behavior of mercury in the cryosphere: A review of what we know
732   from observations, Journal of Geophysical Research: Atmospheres, 116, 10.1029/2010jd014809,
733   2011.

734 Eckley, C. S., Gustin, M., Lin, C. J., Li, X., and Miller, M. B.: The influence of dynamic chamber design
735   and operating parameters on calculated surface-to-air mercury fluxes, Atmospheric Environment, 44,
736   194-203, 10.1016/j.atmosenv.2009.10.013, 2010.

737 Eckley, C. S., Blanchard, P., Mclennan, D., Mintz, R., and Sekela, M.: Soil–air mercury flux near a large
738   industrial emission source before and after closure (Flin Flon, Manitoba, Canada), Environmental
739   Science & Technology, 49, 9750-9757, 2015.

740 Fang, J., Liu, G., Zhu, B., Wang, X., and Liu, S.: Carbon budgets of three temperate forest ecosystems
741   in Dongling Mt., Beijing, China, Science in China Series D-Earth Sciences, 50, 92-101,
742   10.1007/s11430-007-2031-3, 2007.

743 FAO: UNESCO soil map of the world, revised legend, in, World Res. Rep., 138, 1988.

744 Fraser, A., Dastoor, A., and Ryjkov, A.: How important is biomass burning in Canada to mercury
745   contamination?, Atmospheric Chemistry and Physics, 18, 7263-7286, 10.5194/acp-18-7263-2018,
746   2018.

747 Fu, X., Feng, X., and Wang, S.: Exchange fluxes of Hg between surfaces and atmosphere in the eastern
748   flank of Mount Gongga, Sichuan province, southwestern China, Journal of Geophysical Research-
749   Atmospheres, 113, 253-270, 2008.

750 Gao, Y., Wang, Z., Zhang, X., and Wang, C.: Observation and estimation of mercury exchange fluxes
751   from soil under different crop cultivars and planting densities in North China Plain, Environmental
752   pollution, 259, 113833, 10.1016/j.envpol.2019.113833, 2020.

753 Gustin, M. S.: Are mercury emissions from geologic sources significant? A status report, Science of the
754   Total Environment, 304, 153, 2003.

755 Gustin, M. S., and Stamenkovic, J.: Effect of watering and soil moisture on mercury emissions from soils,
756   Biogeochemistry, 76, 215-232, 2005.

757 Gustin, M. S., Engle, M., Ericksen, J., Lyman, S., Stamenkovic, J., and Xin, M.: Mercury exchange
758   between the atmosphere and low mercury containing substrates, Applied Geochemistry, 21, 1913-
759   1923, 2006.

760 Hararuk, O., Obrist, D., and Luo, Y.: Modelling the sensitivity of soil mercury storage to climate-induced
761   changes in soil carbon pools, Biogeosciences, 10, 2393-2407, 2013.

762 Hartman, J. S., Weisberg, P. J., Pillai, R., Ericksen, J. A., Kuiken, T., Lindberg, S. E., Zhang, H., Rytuba,
763   J. J., and Gustin, M. S.: Application of a rule-based model to estimate mercury exchange for three
764   background biomes in the continental United States, Environmental Science & Technology, 43, 4989-
765   4994, 10.1021/es900075q, 2009.

766 Haynes, K. M., Kane, E. S., Potvin, L., Lilleskov, E. A., Kolka, R. K., and Mitchell, C. P. J.: Gaseous
767   mercury fluxes in peatlands and the potential influence of climate change, Atmospheric Environment,
768   154, 247-259, https://doi.org/10.1016/j.atmosenv.2017.01.049, 2017.

769 Hou, H. Y.: Vegetation Map of P.R. China(1:4, 000, 000), Beijing, 1982.

770 Howard, D., and Edwards, G. C.: Mercury fluxes over an Australian alpine grassland and observation of

nocturnal atmospheric mercury depletion events, Atmospheric Chemistry and Physics, 18, 129-142, 10.5194/acp-18-129-2018, 2018.

Johnson, D. W., Benesch, J. A., Gustin, M. S., Schorran, D. S., Lindberg, S. E., and Coleman, J. S.: Experimental evidence against diffusion control of Hg evasion from soils, Science of the Total Environment, 304, 175, 2003.

Kamp, J., Skov, H., Jensen, B., and Sorensen, L. L.: Fluxes of gaseous elemental mercury (GEM) in the High Arctic during atmospheric mercury depletion events (AMDEs), Atmospheric Chemistry and Physics, 18, 6923-6938, 10.5194/acp-18-6923-2018, 2018.

Kiese, R., and Butterbach-Bahl, K.: N2O and CO2 emissions from three different tropical forest sites in the wet tropics of Queensland, Australia, Soil Biology & Biochemistry, 34, 975-987, 2002.

Kocman, D., and Horvat, M.: A laboratory based experimental study of mercury emission from contaminated soils in the River Idrijca catchment, Atmospheric Chemistry and Physics, 10, 1417-1426, 2010.

Kumari, A., Kumar, B., Manzoor, S., and Kulshrestha, U.: Status of Atmospheric Mercury Research in South Asia: A Review, Aerosol and Air Quality Research, 15, 1092-1109, 10.4209/aaqr.2014.05.0098, 2015.

Kuss, J., Krueger, S., Ruickoldt, J., and Wlost, K.-P.: High-resolution measurements of elemental mercury in surface water for an improved quantitative understanding of the Baltic Sea as a source of atmospheric mercury, Atmospheric Chemistry and Physics, 18, 4361-4376, 10.5194/acp-18-4361-2018, 2018.

Li, F., Ma, C., and Zhang, P.: Mercury Deposition, Climate Change and Anthropogenic Activities: A Review, Frontiers in Earth Science, 8, 10.3389/feart.2020.00316, 2020.

Lin, C. J., Gustin, M. S., Singhasuk, P., Eckley, C., and Miller, M.: Empirical models for estimating mercury flux from soils, Environmental Science & Technology, 44, 8522-8528, 2010.

Lin, H., Tong, Y., Yin, X., Zhang, Q., Zhang, H., Zhang, H., Chen, L., Kang, S., Zhang, W., Schauer, J., de Foy, B., Bu, X., and Wang, X.: First measurement of atmospheric mercury species in Qomolangma Natural Nature Preserve, Tibetan Plateau, and evidence of transboundary pollutant invasion, Atmospheric Chemistry and Physics, 19, 1373-1391, 10.5194/acp-19-1373-2019, 2019.

Liu, K., Wu, Q., Wang, L., Wang, S., Liu, T., Ding, D., Tang, Y., Li, G., Tian, H., Duan, L., Wang, X., Fu, X., Feng, X., and Hao, J.: Measure-specific effectiveness of air pollution control on China's atmospheric mercury concentration and deposition during 2013-2017, Environmental Science & Technology, 53, 8938-8946, 10.1021/acs.est.9b02428, 2019.

Luo, Y.: Mercury input, output and transport in forest ecosystems in southern China, Doctor's dissertation, Tsinghua University, Beijing, China, , pp. 1–112 pp., 2015.

Ly Sy Phu, N., Zhang, L., Lin, D.-W., Lin, N.-H., and Sheu, G.-R.: Eight-year dry deposition of atmospheric mercury to a tropical high mountain background site downwind of the East Asian continent, Environmental Pollution, 255, 10.1016/j.envpol.2019.113128, 2019.

Ma, J., Hu, Y., Bu, R., Chang, Y., Deng, H., and Qin, Q.: Predicting Impacts of Climate Change on the Aboveground Carbon Sequestration Rate of a Temperate Forest in Northeastern China, Plos One, 9, 10.1371/journal.pone.0096157, 2014.

Ma, M., Wang, D., Sun, R., Shen, Y., and Huang, L.: Gaseous mercury emissions from subtropical forested and open field soils in a national nature reserve, southwest China, Atmospheric Environment, 64, 116-123, 2013.

Ma, M., Sun, T., Du, H., and Wang, D.: A Two-Year Study on Mercury Fluxes from the Soil under

815   Different Vegetation Cover in a Subtropical Region, South China, Atmosphere, 9,
816   10.3390/atmos9010030, 2018.

817   Manca, G., Ammoscato, I., Esposito, G., Ianniello, A., Nardino, M., and Sprovieri, F.: Dynamics of snow-
818   air mercury exchange at Ny Ålesund during springtime 2011, E3S Web of Conferences, 1, 03010,
819   2013.

820   Maxwell, J. A., Holsen, T. M., and Mondal, S.: Gaseous elemental mercury (GEM) emissions from snow
821   surfaces in northern New York, Plos One, 8, e69342, 2013.

822   Mo, F., Li, X., He, S., and Wang, X.: Evaluation of soil and water conservation capacity of different
823   forest types in Dongling Mountain, Shengtai Xuebao/Acta Ecologica Sinica, 31, 5009-5016, 2011.

824   Nagati, M., Roy, M., DesRochers, A., Bergeron, Y., and Gardes, M.: Importance of soil, stand, and
825   mycorrhizal fungi inabiesbalsameaestablishment in the boreal forest, Forests, 11, 10.3390/f11080815,
826   2020.

827   O'Connor, D., Hou, D., Ok, Y. S., Mulder, J., Duan, L., Wu, Q., Wang, S., Tack, F. M. G., and Rinklebe,
828   J.: Mercury speciation, transformation, and transportation in soils, atmospheric flux, and implications
829   for risk management: A critical review, Environment International, 126, 747-761,
830   10.1016/j.envint.2019.03.019, 2019.

831   Obrist, D., Faïn, X., and Berger, C.: Gaseous elemental mercury emissions and CO(2) respiration rates
832   in terrestrial soils under controlled aerobic and anaerobic laboratory conditions, Science of the Total
833   Environment, 408, 1691-1700, 2010.

834   Obrist, D.: Mercury distribution across 14 U.S. forests. Part II: Patterns of methyl mercury concentrations
835   and areal mass of total and methyl mercury, Environmental Science & Technology, 46, 7434, 2012.

836   Obrist, D., Pokharel, A. K., and Moore, C.: Vertical profile measurements of soil air suggest
837   immobilization of gaseous elemental mercury in mineral soil, Environmental Science & Technology,
838   48, 2242, 2014.

839   Obrist, D., Kirk, J. L., Zhang, L., Sunderland, E. M., Jiskra, M., and Selin, N. E.: A review of global
840   environmental mercury processes in response to human and natural perturbations: Changes of
841   emissions, climate, and land use, Ambio, 47, 116-140, 10.1007/s13280-017-1004-9, 2018.

842   Olson, C., Jiskra, M., Biester, H., Chow, J., and Obrist, D.: Mercury in Active-Layer Tundra Soils of
843   Alaska: Concentrations, Pools, Origins, and Spatial Distribution, Global Biogeochemical Cycles, 32,
844   1058-1073, 10.1029/2017gb005840, 2018.

845   Osterwalder, S., Sommar, J., Akerblom, S., Jocher, G., Fritsche, J., Nilsson, M. B., Bishop, K., and
846   Alewell, C.: Comparative study of elemental mercury flux measurement techniques over a
847   Fennoscandian boreal peatland, Atmospheric Environment, 172, 16-25,
848   10.1016/j.atmosenv.2017.10.025, 2018.

849   Osterwalder, S., Huang, J.-H., Shetaya, W. H., Agnan, Y., Frossard, A., Frey, B., Alewell, C., Kretzschmar,
850   R., Biester, H., and Obrist, D.: Mercury emission from industrially contaminated soils in relation to
851   chemical, microbial, and meteorological factors, Environmental Pollution, 250, 944-952,
852   10.1016/j.envpol.2019.03.093, 2019.

853   Outridge, P. M., Mason, R. P., Wang, F., Guerrero, S., and Heimburger-Boavida, L. E.: Updated global
854   and oceanic mercury budgets for the united nations global mercury assessment 2018, Environmental
855   Science & Technology, 52, 11466-11477, 10.1021/acs.est.8b01246, 2018.

856   Pan, L., Lin, C.-J., Carmichael, G. R., Streets, D. G., Tang, Y., Woo, J.-H., Shetty, S. K., Chu, H.-W., Ho,
857   T. C., Friedli, H. R., and Feng, X.: Study of atmospheric mercury budget in East Asia using STEM-
858   Hg modeling system, Science of the Total Environment, 408, 3277-3291,

859   10.1016/j.scitotenv.2010.04.039, 2010.

860 Pannu, R., Siciliano, S. D., and O'Driscoll, N. J.: Quantifying the effects of soil temperature, moisture
861   and sterilization on elemental mercury formation in boreal soils, Environmental Pollution, 193, 138,
862   2014.

863 Peleg, M., Tas, E., Matveev, V., Obrist, D., Moore, C. W., Gabay, M., and Luria, M.: Observational
864   evidence for involvement of nitrate radicals in nighttime oxidation of mercury, Environmental
865   Science & Technology, 49, 14008, 2015.

866 Perez-Rodriguez, M., Biester, H., Aboal, J. R., Toro, M., and Martinez Cortizas, A.: Thawing of snow
867   and ice caused extraordinary high and fast mercury fluxes to lake sediments in Antarctica,
868   Geochimica Et Cosmochimica Acta, 248, 109-122, 10.1016/j.gca.2019.01.009, 2019.

869 Richardson, J. B., and Friedland, A. J.: Mercury in coniferous and deciduous upland forests in northern
870   New England, USA: implications of climate change, Biogeosciences, 12, 6737-6749, 10.5194/bg-
871   12-6737-2015, 2015.

872 Risch, M. R., DeWild, J. F., Gay, D. A., Zhang, L., Boyer, E. W., and Krabbenhoft, D. P.: Atmospheric
873   mercury deposition to forests in the eastern USA, Environmental Pollution, 228, 8-18,
874   10.1016/j.envpol.2017.05.004, 2017.

875 Slemr, F., Weigelt, A., Ebinghaus, R., Bieser, J., Brenninkmeijer, C. A. M., Rauthe-Schoech, A., Hermann,
876   M., Martinsson, B. G., van Velthoven, P., Boenisch, H., Neumaier, M., Zahn, A., and Ziereis, H.:
877   Mercury distribution in the upper troposphere and lowermost stratosphere according to
878   measurements by the IAGOS-CARIBIC observatory: 2014-2016, Atmospheric Chemistry and
879   Physics, 18, 12329-12343, 10.5194/acp-18-12329-2018, 2018.

880 Sørbotten, L. E.: Hill slope unsaturated flowpaths and soil moisture variability in a forested catchment
881   in Southwest China, MD, Department of Plant and Environmental Sciences, University of Life
882   Sciences, 2011.

883 Spolaor, A., Barbaro, E., Cappelletti, D., Turetta, C., Mazzola, M., Giardi, F., Bjorkman, M. P., Lucchetta,
884   F., Dallo, F., Pfaffhuber, K. A., Angot, H., Dommergue, A., Maturilli, M., Saiz-Lopez, A., Barbante,
885   C., and Cairns, W. R. L.: Diurnal cycle of iodine, bromine, and mercury concentrations in Svalbard
886   surface snow, Atmospheric Chemistry and Physics, 19, 13325-13339, 10.5194/acp-19-13325-2019,
887   2019.

888 St Louis, V. L., Graydon, J. A., Lehnherr, I., Amos, H. M., Sunderland, E. M., St Pierre, K. A., Emmerton,
889   C. A., Sandilands, K., Tate, M., Steffen, A., and Humphreys, E. R.: Atmospheric Concentrations and
890   Wet/Dry Loadings of Mercury at the Remote Experimental Lakes Area, Northwestern Ontario,
891   Canada, Environmental Science & Technology, 53, 8017-8026, 10.1021/acs.est.9b01338, 2019.

892 Sun, T., Ma, M., Wang, X., Wang, Y., Du, H., Xiang, Y., Xu, Q., Xie, Q., and Wang, D.: Mercury transport,
893   transformation and mass balance on a perspective of hydrological processes in a subtropical forest of
894   China, Environmental Pollution, 254, 10.1016/j.envpol.2019.113065, 2019.

895 Teixeira, D. C., Lacerda, L. D., and Silva-Filho, E. V.: Foliar mercury content from tropical trees and its
896   correlation with physiological parameters in situ, Environmental Pollution, 242, 1050-1057,
897   10.1016/j.envpol.2018.07.120, 2018.

898 Wang, Q., Luo, Y., Du, B., Ye, Z., and Duan, L.: Influencing factors of mercury emission flux from forest
899   soil at tieshanping,chongqing, Environmental Science, 35, 1922-1927, 2014.

900 Wang, S., Feng, X., Qiu, G., Fu, X., and Wei, Z.: Characteristics of mercury exchange flux between soil
901   and air in the heavily air-polluted area, eastern Guizhou, China, Atmospheric Environment, 41, 5584-
902   5594, 2007.

Wang, X., Bao, Z., Lin, C.-J., Yuan, W., and Feng, X.: Assessment of global mercury deposition through litterfall, Environmental science & technology, 50, 8548-8557, 2016.

Wang, X., Lin, C.-J., Feng, X., Yuan, W., Fu, X., Zhang, H., Wu, Q., and Wang, S.: Assessment of regional mercury deposition and emission outflow in mainland China, Journal of Geophysical Research-Atmospheres, 123, 9868-9890, 10.1029/2018jd028350, 2018.

Wang, Z., Zhang, X., Xiao, J., Zhijia, C., and Yu, P.: Mercury fluxes and pools in three subtropical forested catchments, southwest China, Environmental Pollution, 157, 801-808, 10.1016/j.envpol.2008.11.018, 2009.

Wang, Z. H., Zhang, G., Wang, Y., Zhao, Y. X., and Sun, X. J.: Research on mercury flux between snow and air under the condition of seasonal snow cover environment, Journal of Agro-Environment Science, 32, 601-606, 2013.

Wright, L. P., Zhang, L., and Marsik, F. J.: Overview of mercury dry deposition, litterfall, and throughfall studies, Atmospheric Chemistry and Physics, 16, 13399-13416, 10.5194/acp-16-13399-2016, 2016.

Wu, Z., Dai, E., Wu, Z., and Lin, M.: Future forest dynamics under climate change, land use change, and harvest in subtropical forests in Southern China, Landscape Ecology, 34, 843-863, 10.1007/s10980-019-00809-8, 2019.

Xin, M., and Gustin, M. S.: Gaseous elemental mercury exchange with low mercury containing soils: Investigation of controlling factors, Applied Geochemistry, 22, 1451-1466, 2007.

Yu, Q., Luo, Y., Xu, G., Wu, Q., Wang, S., Hao, J., and Duan, L.: Subtropical forests act as mercury sinks but as net sources of gaseous elemental mercury in south China, Environmental Science & Technology, 54, 2772-2779, 10.1021/acs.est.9b06715, 2020.

Yuan, W., Sommar, J., Lin, C.-J., Wang, X., Li, K., Liu, Y., Zhang, H., Lu, Z., Wu, C., and Feng, X.: Stable Isotope Evidence Shows Re-emission of Elemental Mercury Vapor Occurring after Reductive Loss from Foliage, Environmental Science & Technology, 53, 651-660, 10.1021/acs.est.8b04865, 2019a.

Yuan, W., Wang, X., Lin, C.-J., Sommar, J., Lu, Z., and Feng, X.: Process factors driving dynamic exchange of elemental mercury vapor over soil in broadleaf forest ecosystems, Atmospheric Environment, 219, 10.1016/j.atmosenv.2019.117047, 2019b.

Zarate-Valdez, J. L., Zasoski, R. J., and Lauchli, A.: Short-term effects of moisture content on soil solution pH and soil Eh, Soil Science, 171, 423-431, 10.1097/01.ss.0000222887.13383.08, 2006.

Zhang, G., Wang, N., Ai, J.-C., Zhang, L., Yang, J., and Liu, Z.-Q.: Characteristics of mercury exchange flux between soil and atmosphere under the snow retention and snow melting control, Huan jing ke xue= Huanjing kexue, 34, 468-475, 2013.

Zhang, H., Lindberg, S. E., Marsik, F. J., and Keeler, G. J.: Mercury air/surface exchange kinetics of background soils of the tahquamenon river watershed in the Michigan Upper Peninsula, Water Air & Soil Pollution, 126, 151-169, 2001.

Zhang, H., Lindberg, S. E., Barnett, M. O., Vette, A. F., and Gustin, M. S.: Dynamic flux chamber measurement of gaseous mercury emission fluxes over soils. Part 1: simulation of gaseous mercury emissions from soils using a two-resistance exchange interface model, Atmospheric Environment, 36, 835-846, 2002.

Zhang, H., Nizzetto, L., Feng, X., Borga, K., Sommar, J., Fu, X., Zhang, H., Zhang, G., and Larssen, T.: Assessing Air-Surface Exchange and Fate of Mercury in a Subtropical Forest Using a Novel Passive Exchange-Meter Device, Environmental Science & Technology, 53, 4869-4879, 10.1021/acs.est.8b06343, 2019a.

947 Zhang, L., Zhou, P., Cao, S., and Zhao, Y.: Atmospheric mercury deposition over the land surfaces and
948   the associated uncertainties in observations and simulations: a critical review, Atmospheric
949   Chemistry and Physics, 19, 15587-15608, 10.5194/acp-19-15587-2019, 2019b.

950 Zhang, Q., Huang, J., Wang, F., Mark, L., Xu, J., Armstrong, D., Li, C., Zhang, Y., and Kang, S.: Mercury
951   distribution and deposition in glacier snow over western China, Environmental science & technology,
952   46, 5404, 2012.

953 Zhou, J., Wang, Z., Zhang, X., and Chen, J.: Distribution and elevated soil pools of mercury in an acidic
954   subtropical forest of southwestern China, Environmental Pollution, 202, 187-195,
955   10.1016/j.envpol.2015.03.021, 2015.

956 Zhou, J., Wang, Z., Sun, T., Zhang, H., and Zhang, X.: Mercury in terrestrial forested systems with highly
957   elevated mercury deposition in southwestern China: The risk to insects and potential release from
958   wildfires, Environmental Pollution, 212, 188-196, 10.1016/j.envpol.2016.01.003, 2016.

959 Zhou, J., Wang, Z., Zhang, X., and Gao, Y.: Mercury concentrations and pools in four adjacent coniferous
960   and deciduous upland forests in Beijing, China, Journal of Geophysical Research: Biogeosciences,
961   122, 1260-1274, 2017a.

962 Zhou, J., Wang, Z., Zhang, X., and Sun, T.: Investigation of factors affecting mercury emission from
963   subtropical forest soil: A field controlled study in southwestern China, Journal of Geochemical
964   Exploration, 176, 128-135, 10.1016/j.gexplo.2015.10.007, 2017b.

965 Zhou, J., Wang, Z., and Zhang, X.: Deposition and fate of mercury in litterfall, litter, and soil in coniferous
966   and broad-leaved forests, Journal of Geophysical Research: Biogeosciences, 123, 2590-2603,
967   10.1029/2018jg004415, 2018.

968 Zhou, J., Du, B., Shang, L., Wang, Z., Cui, H., Fan, X., and Zhou, J.: Mercury fluxes, budgets, and pools
969   in forest ecosystems of China: A review, Critical Reviews in Environmental Science and Technology,
970   50, 1411-1450, 2020.

971 Zhou, J., Wang, Z., Zhang, X., and Driscoll, C. T.: Measurement of vertical distribution of gaseous
972   elemental mercury concentration in soil pore air at subtropical and temperate forests, in review.

973 Zhu, W., Lin, C. J., Wang, X., Sommar, J., Fu, X., and Feng, X.: Global observations and modeling of
974   atmosphere-surface exchange of elemental mercury: a critical review, Atmospheric Chemistry &
975   Physics, 16, 4451-4480, 2016.

976

977   **Table 1.** Locations and summary of measurements (mean ± standard deviation) of soil-air TGM fluxes and environmental parameters at ten plots at the subtropical and

978   temperate forests.

Forest	Plots	Locations	Flux (ng m^{-2} hr^{-1})	Soil surface TGM (ng m^{-3})	Soil Hg concentration (ng g^{-1})	SOM (0-5, %)	Soil moisture (%)	Soil temperature (°C)	Solar radiation (W m^{-2})
Subtropical forest	Plot S-A	Top-slope of coniferous forest	2.8 ± 3.9	3.6±1.3	219±15	13.6	0.3±0.1	16.8±7.6	39.9±27.5
	Plot S-B	Middle-slope of coniferous forest	3.5 ± 4.2	3.8±1.3	263±22	16.3	0.4±0.1	16.9±7.7	40.2±27.5
	Plot S-C	Wetland	-0.80 ± 5.1	3.7±1.4	96±43	4.9	0.3±0.1	16.7±7.5	30.5±27.9
	Plot S-D	Broad-leaved forest	0.18 ± 4.3	3.3±1.4	156±17	8.8	0.3±0.1	16.9±7.6	20.3±27.9
	Plot S-E	Open field	24 ± 33	4.1±1.7	159±18	4.1	0.3±0.1	18.3±8.5	98.0±138.4
Temperate forest	Plot T-A	Chinese pine forest	-0.04±0.81	2.22±0.87	72±12	5.8	17.0±8.55	9.77±6.57	17.09±29.4
	Plot T-B	Larch forest	0.32±0.96	2.30±0.94	141±15	25	26.3±6.51	10.0±6.23	22.9±18.6
	Plot T-C	Wetland	3.81±0.52	2.47±0.92	156±21	47	42.9±8.22	10.0±6.55	22.1±19.4
	Plot T-D	Mixed broad-leaved forest	0.68±1.01	2.37±0.87	74±9	16	25.4±7.32	9.86±6.26	25.9±18.6
	Plot T-E	Open field	1.82±0.79	1.98±0.79	52±4	12	27.9±5.56	10.1±6.47	47.1±29.4

979

980

Figure captions:

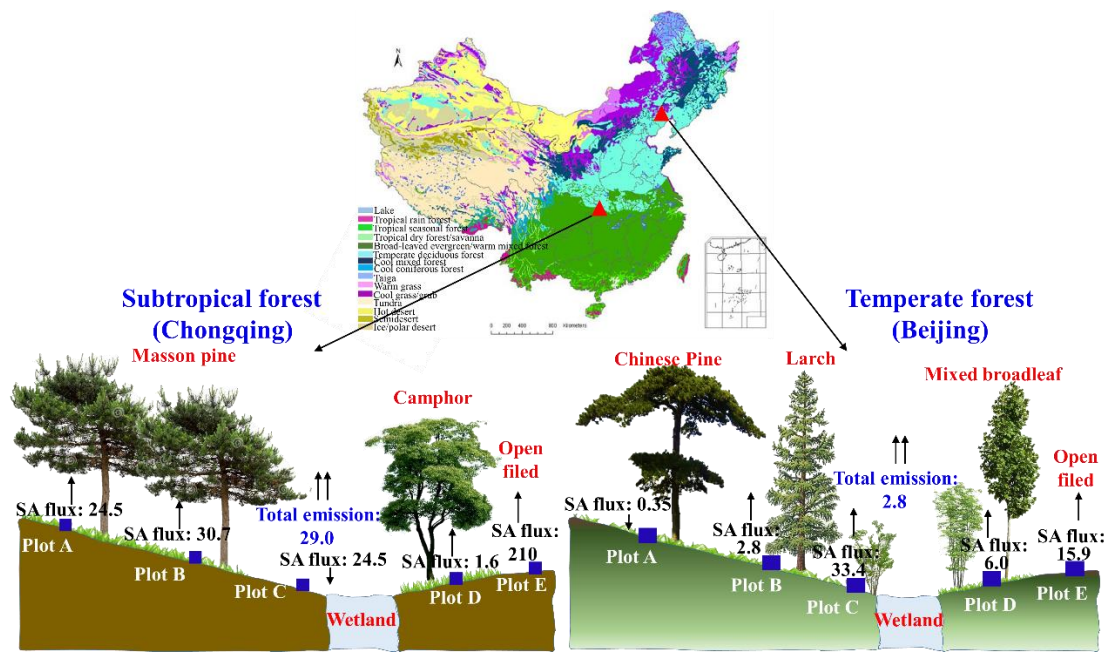**Fig. 1.** Location of the five sampling plots and the estimation of soil-air fluxes (SA fluxes, values as g m^{-2} yr^{-1}) at the temperate and subtropical forest. Potential vegetation of China is from the Vegetation Map of China (Hou, 1982). Up and down arrows represent emission and deposition, respectively.
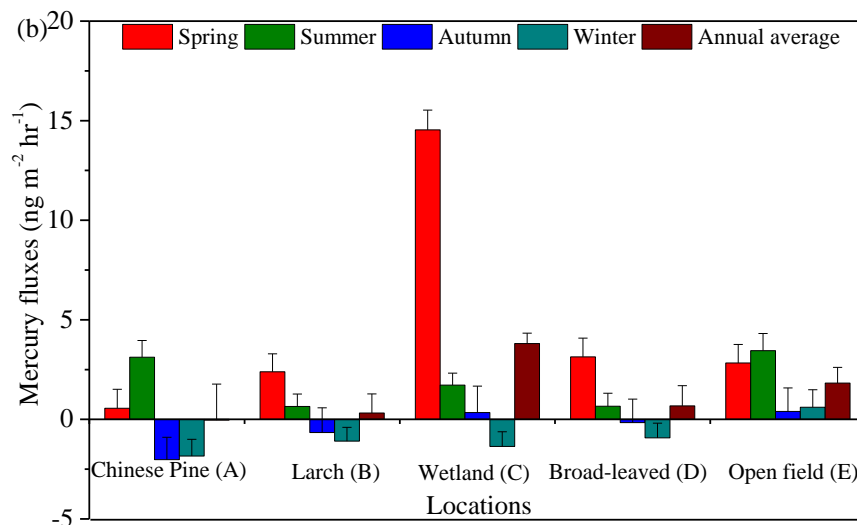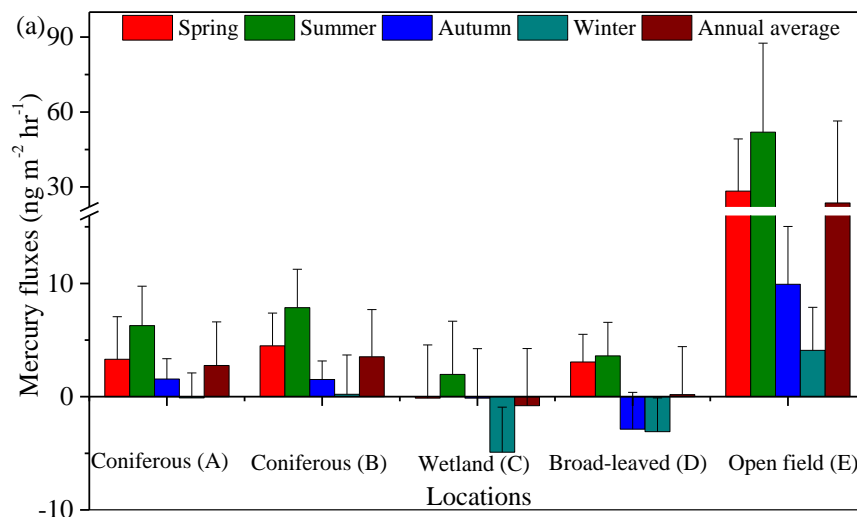
Fig. 2. Mean and standard deviations of soil-air TGM fluxes at the five plots for the four seasons and annual values during the study at the subtropical forest (A) and temperate forest (B). The number of flux observations in spring, summer, autumn and winter were 62, 92, 66 and 43 at the subtropical forest and 60, 58, 60 and 14 for the temperate forest, respectively.
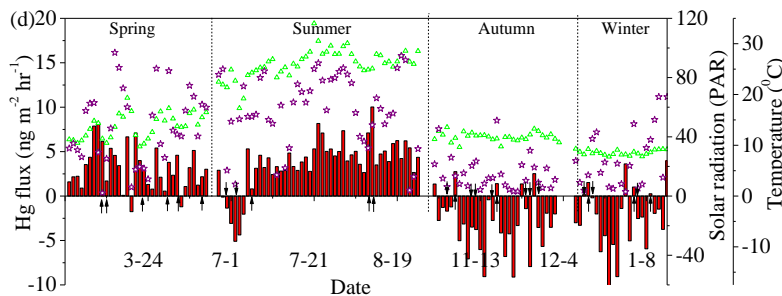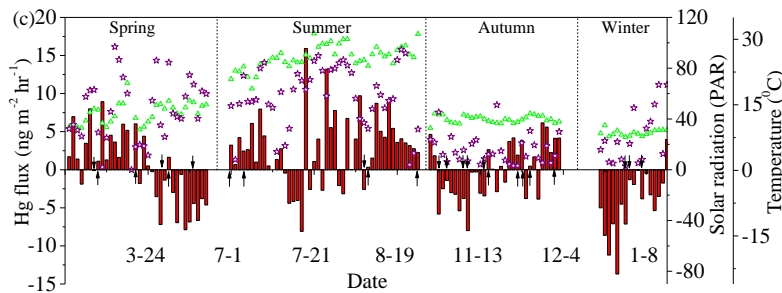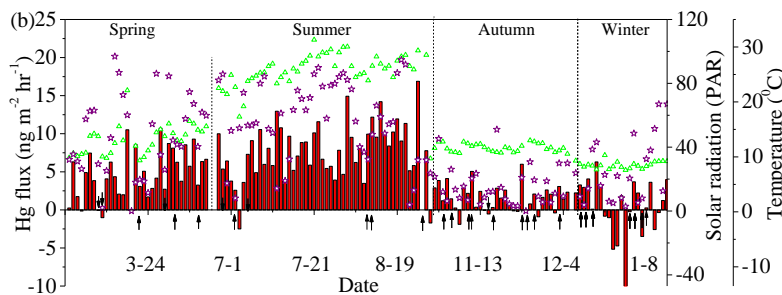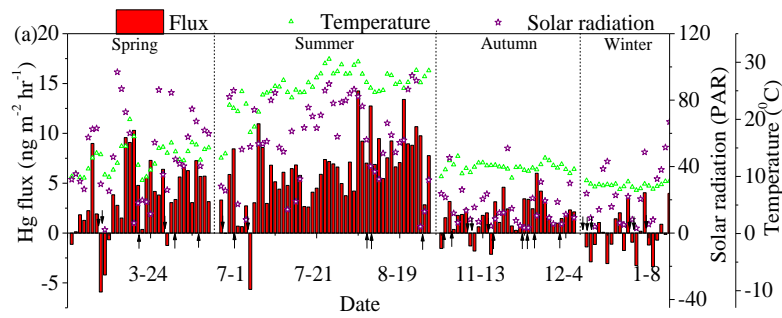
Fig. 3. Daily (average flux of day and night) composite Hg flux, solar radiation and soil temperature at Masson pine forests plots ((A) and (B)), wetland (C), evergreen broad-leaved forest (D) and open field (E) plots at the subtropical forest. The vertical arrows represent precipitation events.
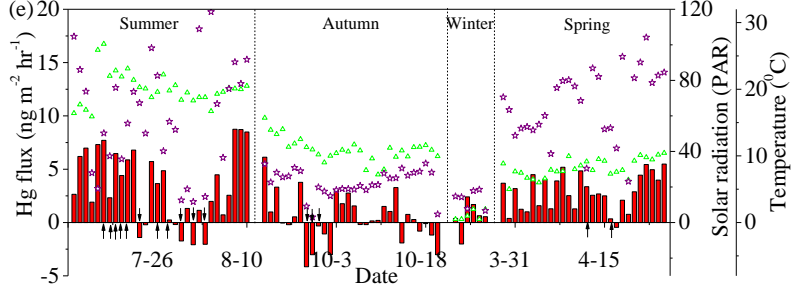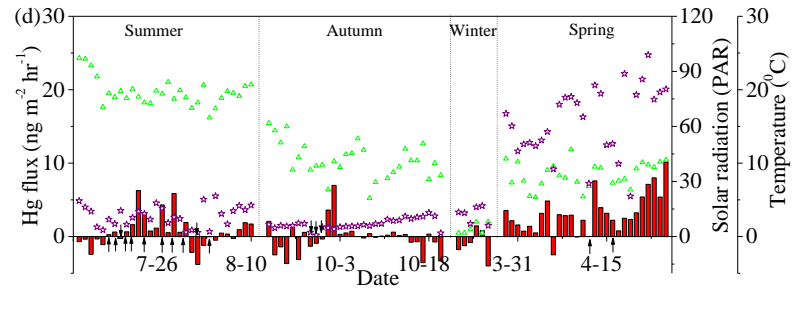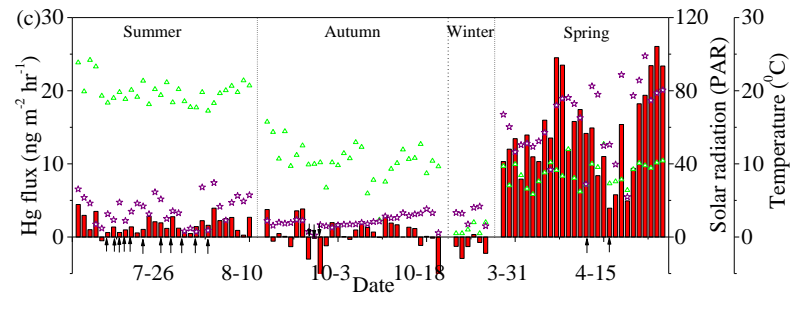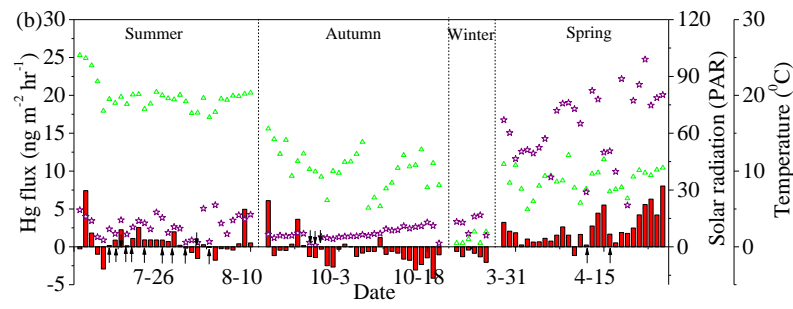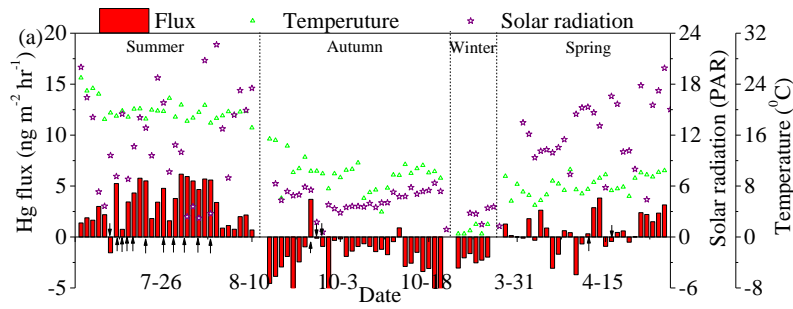
Fig. 4. Daily (average flux of day and night) composite Hg flux, solar radiation and soil temperature at Chinese pine forest (A), larch forest (B), wetland (C), mixed broad-leaved forest (D) and open field (E) plots at the temperate forest. The vertical arrows represent precipitation events.
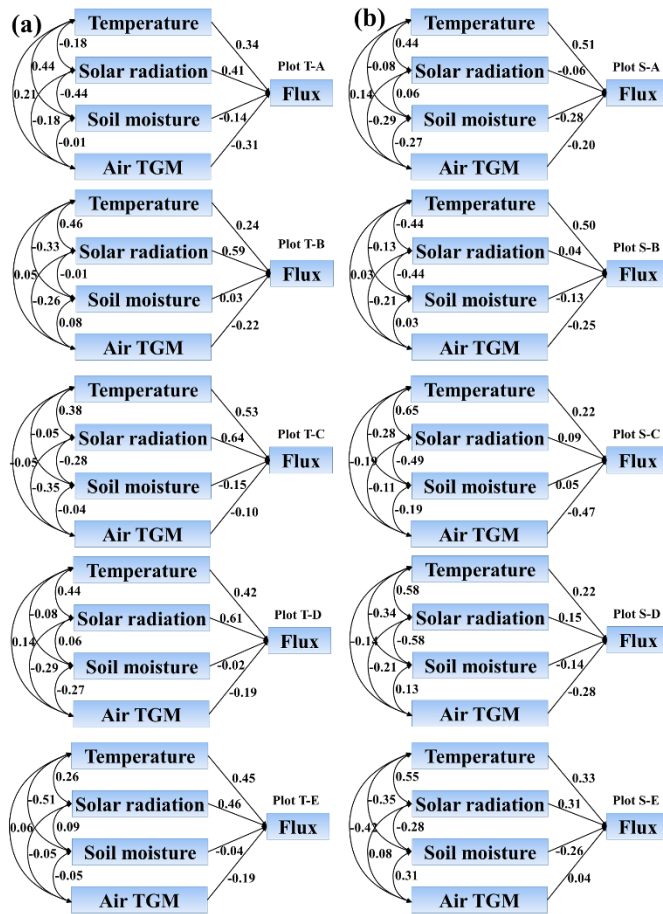
Fig. 5. Interplays of environmental factors on air-soil TGM exchange flux obtained by structural equation model (SEM) in the temperate (a) and subtropical (b) forests.
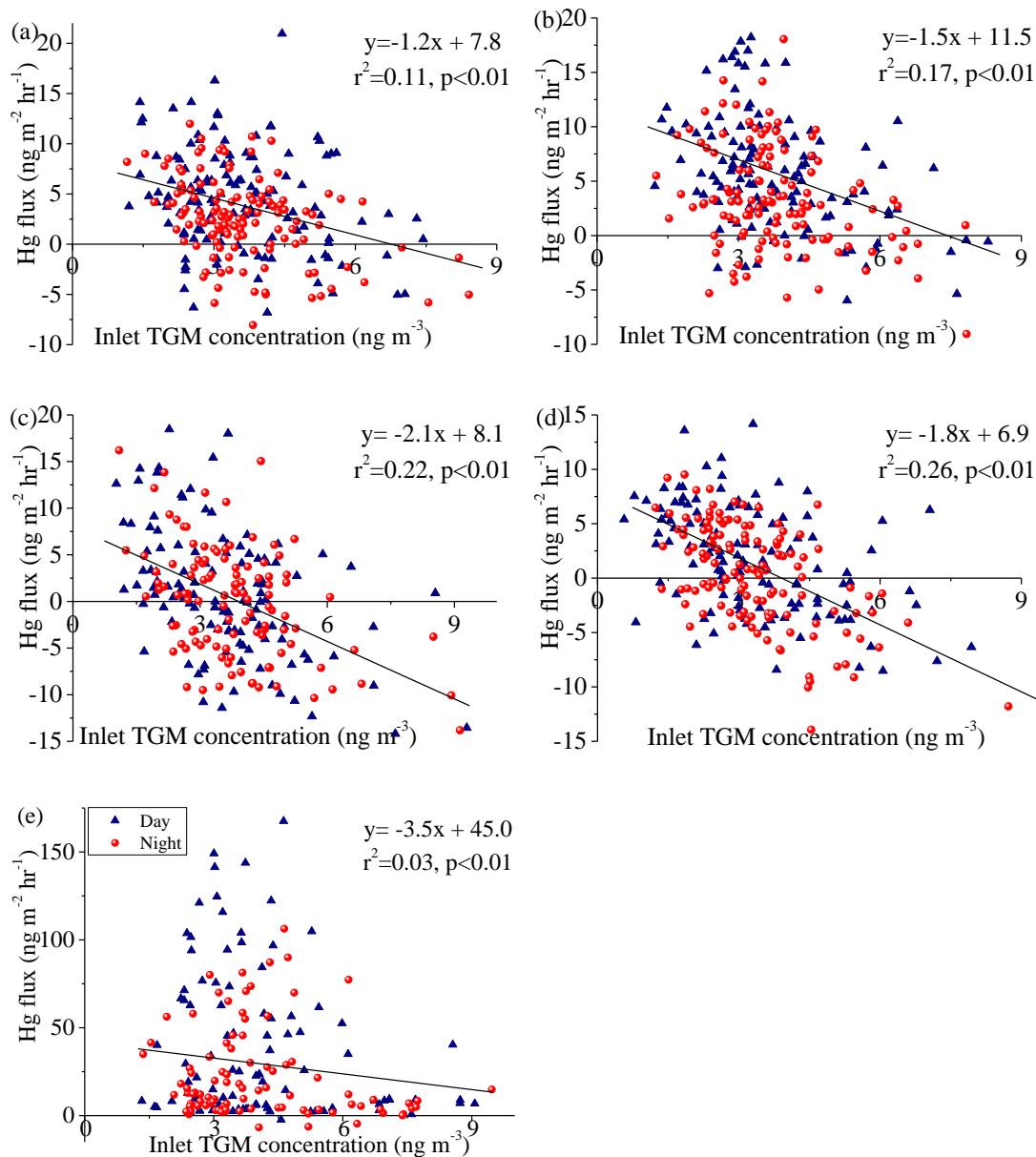
Fig. 6. Correlation between the air TGM concentration and air-surface Hg flux measured in daytime and night over four seasons for at Masson pine forest plots ((A) and (B)), wetland (C), evergreen broad-leaved forest (D) and open field (E) plots at the subtropical forest.

Fig. 7. Correlation between the air TGM concentration and air-surface Hg flux measured in daytime and night over four seasons for the five plots at Chinese pine forest (a), larch forest (b), wetland (c), mixed broad-leaved forest (d) and open field (e) plots at the temperate forest.

Fig. 8. Diurnal patterns of soil Hg fluxes with meteorological parameters in spring (a), summer (b), autumn (c) and winter (d) at the coniferous forest of the subtropical forest.

Fig. 9. Diurnal patterns of soil Hg fluxes with meteorological parameters in spring (a), summer (b), autumn (c) and winter (d) at the deciduous broad-leaved forest of the temperate forest.

1008

Fig. 1. Location of the five sampling plots and the estimation of soil-air fluxes (SA fluxes, values as g m^{-2} yr^{-1}) at the temperate and subtropical forest. Potential vegetation of China is from the Vegetation Map of China (Hou, 1982). Up and down arrows represent emission and deposition, respectively.

Fig. 2. Mean and standard deviations of soil-air TGM fluxes at the five plots for the four seasons and annual values during the study at the subtropical forest (A) and temperate forest (B). The number of flux observations in spring, summer, autumn and winter were 62, 92, 66 and 43 at the subtropical forest and 60, 58, 60 and 14 for the temperate forest, respectively.

Fig. 3. Daily (average flux of day and night) composite Hg flux, solar radiation and soil temperature at Masson pine forests plots ((A) and (B)), wetland (C), evergreen broad-leaved forest (D) and open field (E) plots at the subtropical forest. The vertical arrows represent precipitation events.
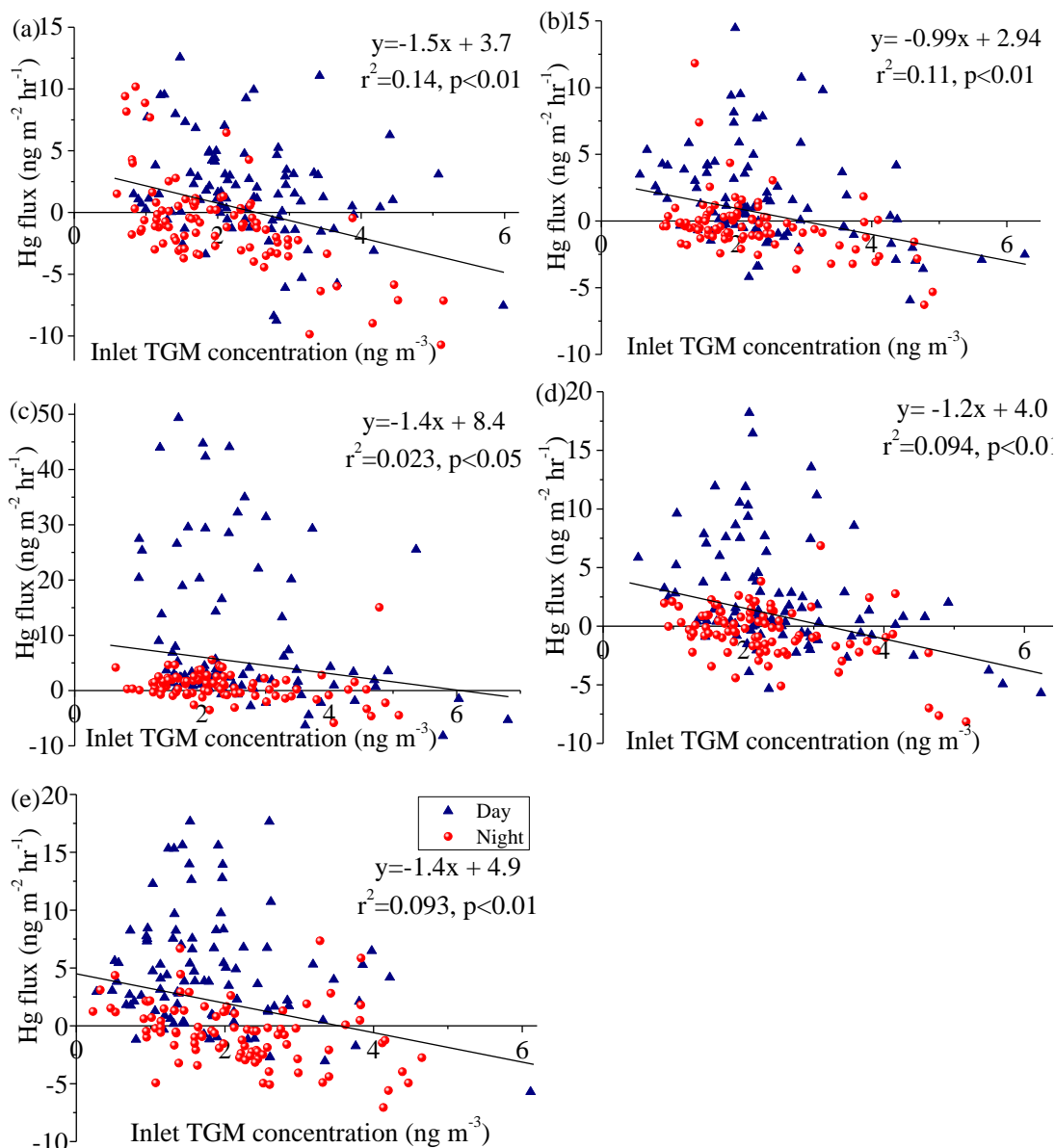
Fig. 4. Daily (average flux of day and night) composite Hg flux, solar radiation and soil temperature at Chinese pine forest (A), larch forest (B), wetland (C), mixed broad-leaved forest (D) and open field (E) plots at the temperate forest. The vertical arrows represent precipitation events.
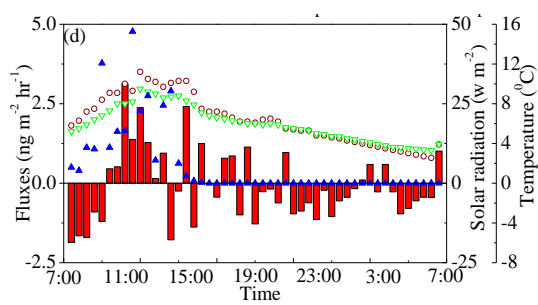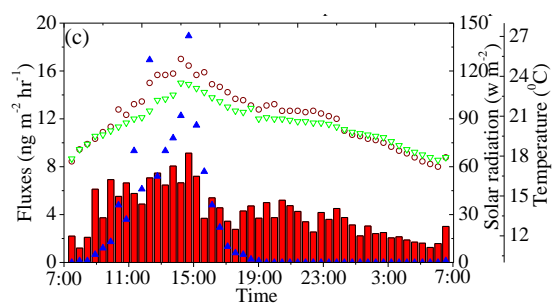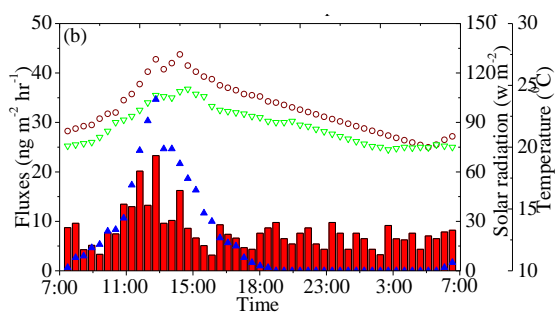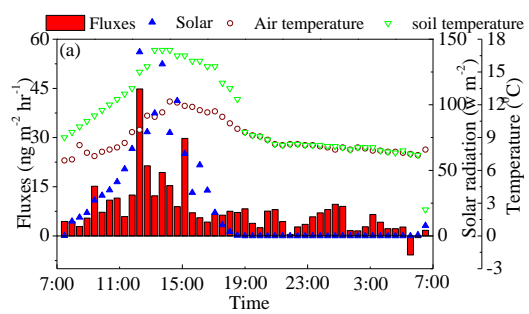
Fig. 5. Interplays of environmental factors on air-soil TGM exchange flux obtained by structural equation model (SEM) in the temperate (a) and subtropical (b) forests.

1044

1045

1046

Fig. 6. Correlation between the air TGM concentration and air-surface Hg flux measured in daytime
and night over four seasons for at Masson pine forest plots ((A) and (B)), wetland (C), evergreen
broad-leaved forest (D) and open field (E) plots at the subtropical forest.

1047
1048
1049
1050

Fig. 7. Correlation between the air TGM concentration and air-surface Hg flux measured in daytime and night over four seasons for the five plots at Chinese pine forest (a), larch forest (b), wetland (c), mixed broad-leaved forest (d) and open field (e) plots at the temperate forest.
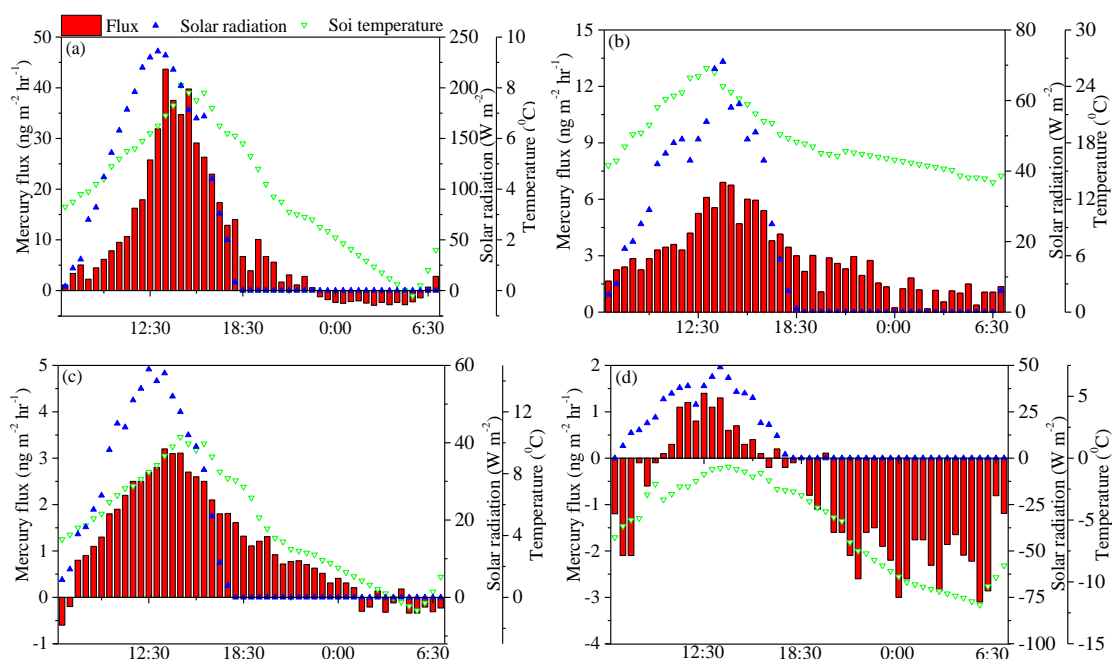
1051

1052

1053

1054

1055

1056

1057

Fig. 8. Diurnal patterns of soil Hg fluxes with meteorological parameters in spring (a), summer (b), autumn (c) and winter (d) at the coniferous forest of the subtropical forest.

Fig. 9. Diurnal patterns of soil Hg fluxes with meteorological parameters in spring (a), summer (b), autumn (c) and winter (d) at the deciduous broad-leaved forest of the temperate forest.

Supporting Information

Soil-atmosphere exchange flux of total gaseous mercury (TGM) at subtropical and temperate forest catchments

Jun Zhou [a, b, c, f], Zhangwei Wang [a, c, *], Xiaoshan Zhang [a, c], Charles T. Driscoll [d], Che-Jen Lin [e]

a. State Key Laboratory of Urban and Regional Ecology, Research Center for Eco-Environmental Sciences, Chinese Academy of Sciences, Beijing 100085, China.

b. Key Laboratory of Soil Environment and Pollution Remediation, Institute of Soil Science, Chinese Academy of Sciences, Nanjing 210008, China.

c. University of Chinese Academy of Sciences, Beijing 100049, China.

d. Department of Civil and Environmental Engineering, Syracuse University, 151 Link Hall, Syracuse, New York 13244, United States.

e. Center for Advances in Water and Air Quality, Lamar University, Beaumont, Texas 77710, United States.

f. Department of Environmental, Earth and Atmospheric Sciences, University of Massachusetts, Lowell, 01854, USA

* Corresponding author: Zhangwei Wang

E-mail address: wangzhw@rcees.ac.cn(Z. Wang); Phone: +86 10 62849168.

No.18 Shuangqing Road, Beijing 100085, China

First author e-mail: zhoujun@issas.ac.cn (J. Zhou); Phone: +86 25 86881319.

No.73 East Beijing Road, Nanjing 210008, China.

Contents:

   19 Pages

   1 Tables

   12 Figures

Supporting Text:

Site description

  In the subtropical forest, the mean annual precipitation, temperature and daily relative humidity at the TFP are 1230 mm, 18.2 °C and 95%, respectively. The ecosystem type at the TFP study site is a Masson Pine dominated forest, with some associated ever-green broad-leaved species. Trees were planted in the 1960s. The soil is typically mountain yellow earth (corresponding to a Haplic Acrisol in FAO). The soil is acidic, with a pH of 3.79. From previous studies, the mean Hg concentrations in precipitation, throughfall, litterfall and organic soils were 55.3 ng L^{-1}, 98.9 ng L^{-1}, 104.8±18.6 ng g^{-1} and 191 ± 65 ng g^{-1}, respectively, with an annual Hg input of 291.2 μg m^{-2} yr^{-1} (Zhou et al., 2016;Zhou et al., 2015).

  The temperate forest is located in the Xiaolongmen National Forest Park of Mt. Dongling near the Beijing Forest Ecosystem Research Station, Chinese Academy of Sciences (40°00′ N, 115°26′ E), which is located 110 km southwest of Mega-city Beijing in North China. The elevation and is 1300 m asl. The annual average rainfall is 612 mm and mean relative humidity is 66%. The Mt. Dongling is one of the Chinese Ecosystem Research Network (CERN) and Diversitas Western Pacific and Asia (DIWPA) monitoring sites. The region's climate is predominantly warm temperate continent monsoon climate with an annual average temperature 4.8 °C. Cool and dry climate in the study area has resulted in deep litter and high organic matter concentrations (Fang et al., 2007). The study area is a mature and secondary forest protected since the 1950s following the extensive deforestation. To characterize the terrestrial surface influence on the Hg fluxes, different ecosystems were selected to study the air-surface Hg fluxes from forest soil and snow at a sub-catchment (40 ha) in the temperate forest, including the Chinese pine forest, larch forest, wetland, mixed broad-leaved forest and open field. The five sites were located about 200-300 m distance individually. From previous studies, the mean litterfall Hg concentrations were 15.8, 19.6, and 12.1 ng g^{-1} in Chinese pine forest, larch forest, and mixed broad-leaved forest plots and the mean soil Hg concentrations (0-5 cm) were 72±12, 141±15, and 74±9 ng g^{-1} in Chinese pine forest, larch forest, and mixed broad-leaved forest, respectively (Zhou et al., 2017).

Environmental measurements

  Daily meteorological parameters were collected and averaged over 5-min intervals. Daily air temperature and solar radiation were monitored using a TP 101 digital thermometer and a GLZ−C photo synthetically radiometer (TOP Ltd. China), respectively, during diurnal measurements. Soil percent moisture and soil temperature at 0-5 cm was monitored with Time Domain Reflectometry (TDR) Hydra Probe II (SDI−12/RS485) and a Stevens water cable tester (USA). Measurements were taken at the same time with gold trap collection. Solar radiation was collected with a weather station (Davis Wireless Vantage VUE 06250 Weather Station, Davis Instruments, Hayward, CA) located in the TFP Forest Station about 500 m away from the sub-catchment.

  For each DFC sampling location, bulk soil samples were collected from the DFC footprints

1136   (0−5 cm) in each month of study after the end of the measurement period. Soil samples were dried

1137   and homogenized, and completely ground to a fine powder in a pre-cleaned stainless-steel blender.

1138   The total Hg concentration in the soil samples was determined using a DMA-80 direct Hg analyzer

1139   (Milestone Ltd., Italy). SOM content in soils was determined using the sequential loss on ignition

1140   (LOI) method.(Zhou et al., 2013) A homogenized soil sample (WS) was dried at 105 °C for about

1141   12- 24 h to obtain the dry weight of the samples (DW_{105}). The heated dry sample was then

1142   combusted at 550 °C for 4 h and the weight of the sample after heating at 550 °C was DW_{550}. Thus,

1143   the TOM concentration (LOI_{550}) was calculated according to the following formula:

1144 $LOI_{550} = 100(DW_{105} - DW_{550})/WS$.

1145 **Table S1.** Characteristics and detail of measurements at five plots in the forested sub-catchments.

Forest type	Plots	Locations	Date of flux measurement				Area (%)
			Spring	Summer	Autumn	Winter	
Subtropical forest	Plot S-A	Top-slope of coniferous forest	5 Mar-7 Apr	17 -19 Jun; 1-31 Jul; 10-24 Aug	3 Nov-6 Dec	24 Dec-14 Jan	42.4
	Plot S-B	Middle-slope of the coniferous forest	5 Mar-7 Apr	17 -19 Jun; 1-31 Jul; 10-24 Aug	3 Nov-6 Dec	24 Dec-14 Jan	42.4
	Plot S-C	Wetland	5 Mar-7 Apr	1-31 Jul; 10-24 Aug	3 Nov-6 Dec	31 Dec-14 Jan	2.9
	Plot S-D	Broad-leaved forest	5 Mar-7 Apr	17 -19 Jun; 1-31 Jul; 10-24 Aug	3 Nov-6 Dec	24 Dec-14 Jan	10
	Plot S-E	Open field	22 Mar-7 Apr	17 -19 Jun; 1-31 Jul; 10-24 Aug	3-23 Nov	30 Dec-14 Jan	2.3
Temperate forest	Plot T-A	Chinese pine forest	28 Mar–25 Apr	12 Jul–10 Aug	20 Sep–20 Oct	10–16 Nov	14
	Plot T-B	Larch forest	28 Mar–25 Apr	12 Jul–10 Aug	20 Sep–20 Oct	10–16 Nov	8
	Plot T-C	Wetland	28 Mar–25 Apr	12 Jul–10 Aug	20 Sep–20 Oct	10–16 Nov	9
	Plot T-D	Mixed broad-leaved forest	28 Mar–25 Apr	12 Jul–10 Aug	20 Sep–20 Oct	10–16 Nov	65
	Plot T-E	Open field	28 Mar–25 Apr	12 Jul–10 Aug	20 Sep–20 Oct	10–16 Nov	4

1146 Note: Area percent was according to Zhu et al. (2013) at the subtropical forest and Zhou et al. (1999) at the temperate forest.
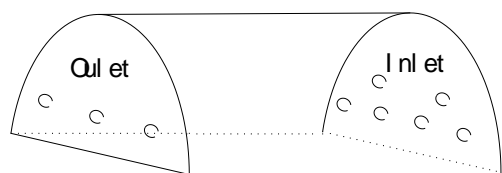
Figure Captions:

1147

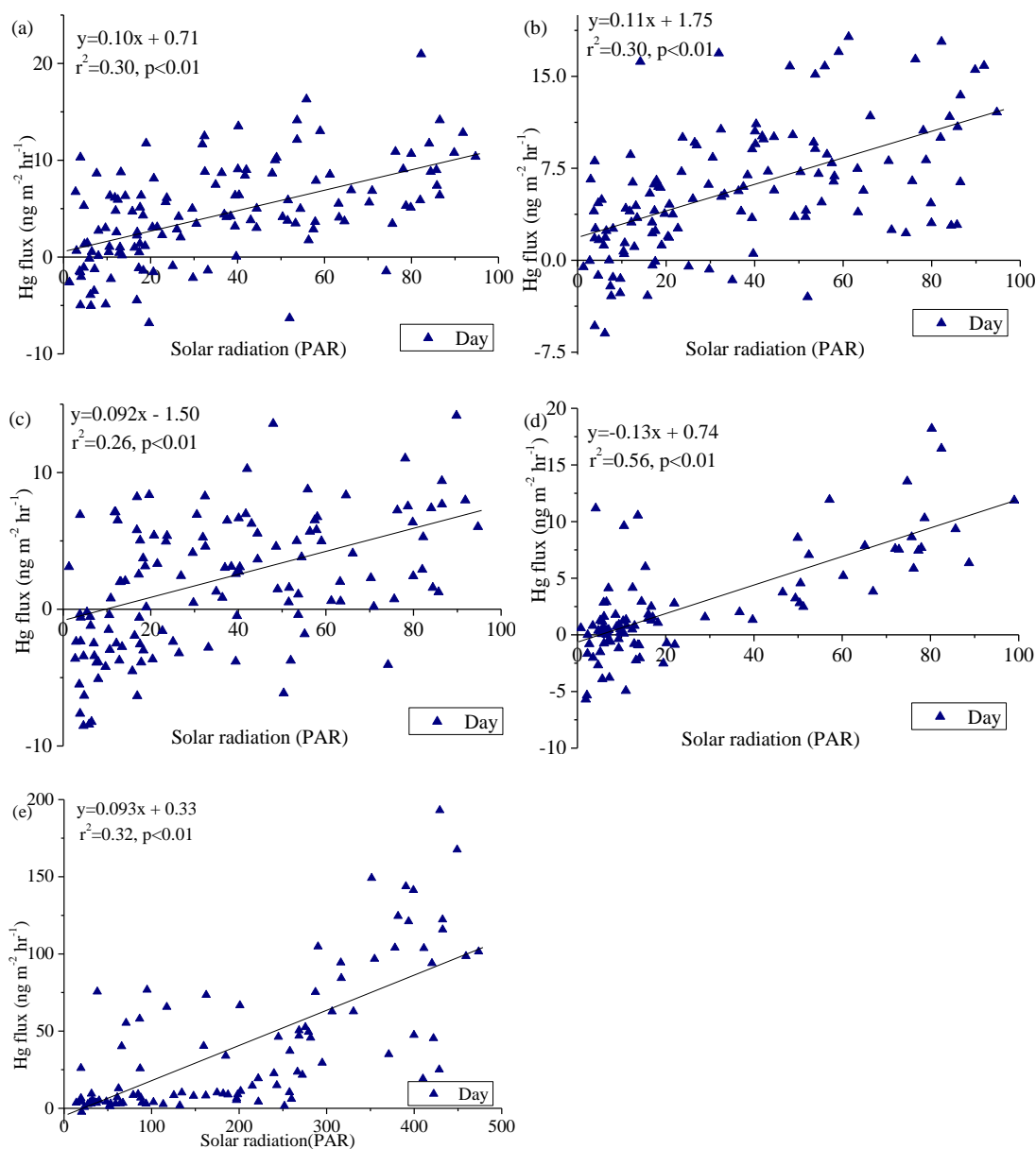1148 **Fig. S1.** Schematic diagram of the dynamic flux chamber used in this study.

1149 **Fig. S2.** Correlations between the averaged solar radiation (8:00-17:00) and air-surface Hg flux

1150 measured during daytime in Masson pine forests (a) and (b), wetland (c), evergreen broad-leaved

1151 forest (d) and open field (e) in the subtropical forest.

1152 **Fig. S3.** Correlation between the averaged solar radiation (8:00-17:00) and air-surface Hg flux

1153 measured during daytime in Chinese pine forest (a), larch forest (b), wetland (c), mixed broad-

1154 leaved forest (d) and open field (e) in the temperate forest.

1155 **Fig. S4.** Effects of rainfall events on annual soil-air TGM fluxes at Masson pine forests (Plot A) and

1156 (Plot B), wetland (Plot C), evergreen broad-leaved forest (Plot D) and open field (Plot E) at the

1157 subtropical forest (A), and at Chinese pine forest (Plot A), larch forest (Plot B), wetland (Plot C),

1158 mixed broad-leaved forest (Plot D) and open field (Plot E) at the temperate forest (B).

1159 **Fig. S5.** Correlation between the soil Hg concentrations ($S_c \pm SD$) and soil-air Hg flux ($F \pm SD$)

1160 under the forest canopy at the subtropical forest. Standard deviations of soil Hg concentrations

1161 were obtained from Hg concentrations over the four seasons (n=12). Because fluxes are often

1162 controlled by solar radiation for bare soils, the correlation analysis above does not include data

1163 from the open field (plot E).

1164 **Fig. S6.** Soil-air TGM fluxes during the daytime and nighttime at Masson pine forests (Plot A) and

1165 (Plot B), wetland (Plot C), evergreen broad-leaved forest (Plot D) and open field (Plot E) at the

1166 subtropical forest (a), and at Chinese pine forest (Plot A), larch forest (Plot B), wetland (Plot C),

1167 mixed broad-leaved forest (Plot D) and open field (Plot E) at the temperate forest (b).

1168 **Fig. S7.** Correlations between soil temperature and air-surface Hg fluxes measured during daytime

1169 and night at the Masson pine forests (a) and (b), wetland (c), evergreen broad-leaved forest (d)

1170 and open field (e) in the subtropical forest.

1171 **Fig. S8.** Correlations between soil temperature and air-surface Hg fluxes measured during daytime

1172 and night at the Chinese pine forest (a), larch forest (b), wetland (c), mixed broad-leaved forest

1173 (d) and open field (e) at the temperate forest.

1174 **Fig. S9.** Correlations between soil moisture and air-surface Hg fluxes measured during daytime and

1175   night at the Chinese pine forest (a), larch forest (b), wetland (c), mixed broad-leaved forest (d)

1176   and open field (e) at the subtropical forest.

1177 **Fig. S10.** Correlations between soil moisture and air-surface Hg fluxes measured during daytime

1178   and night at the Chinese pine forest (a), larch forest (b), wetland (c), mixed broad-leaved forest

1179   (d) and open field (e) at the temperate forest.

1180 **Fig. S11.** Correlations between the gradient of Hg(0) concentrations between surface soil pore (at 3

1181   cm) and atmospheric values and soil-air Hg(0) flux at four plots at the subtropical forest.

1182 **Fig. S12.** Correlations between the gradient of Hg(0) concentrations between surface soil pore (at 3

1183   cm) and atmospheric values and soil-air Hg(0) flux at the four plots at the temperate forest.

1184

1185

1186

1187   **Fig. S1.** Schematic diagram of the dynamic flux chamber used in this study.

1188

1189

Fig. S2. Correlations between the averaged solar radiation (8:00-17:00) and air-surface Hg flux measured during daytime in Masson pine forests (a) and (b), wetland (c), evergreen broad-leaved forest (d) and open field (e) in the subtropical forest.
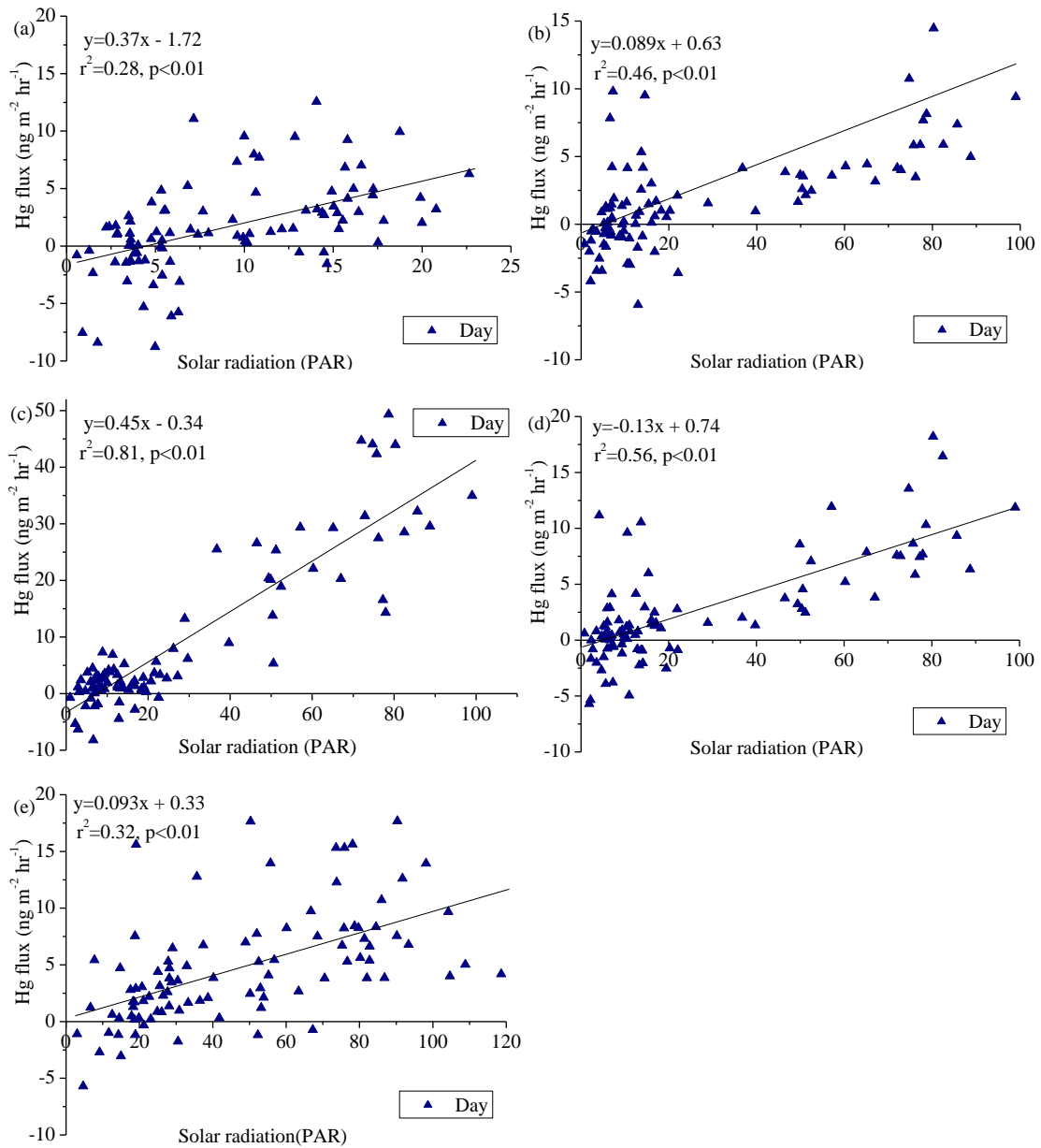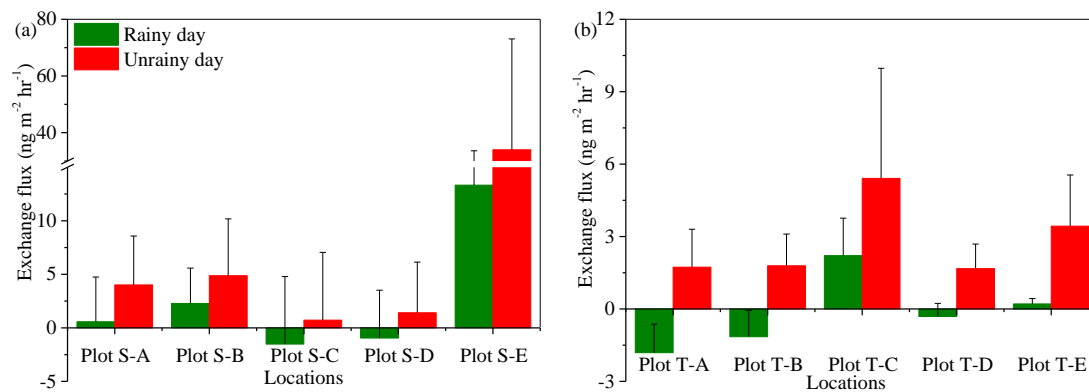
1197

1198

1199

1200 **Fig. S3.** Correlation between the averaged solar radiation (8:00-17:00) and air-surface Hg flux
1201 measured during daytime in Chinese pine forest (a), larch forest (b), wetland (c), mixed broad-
1202 leaved forest (d) and open field (e) in the temperate forest.

1203

Fig. S4. Effects of rainfall events on annual soil-air TGM fluxes at Masson pine forests (Plot A) and (Plot B), wetland (Plot C), evergreen broad-leaved forest (Plot D) and open field (Plot E) at the subtropical forest (A), and at Chinese pine forest (Plot A), larch forest (Plot B), wetland (Plot C), mixed broad-leaved forest (Plot D) and open field (Plot E) at the temperate forest (B).
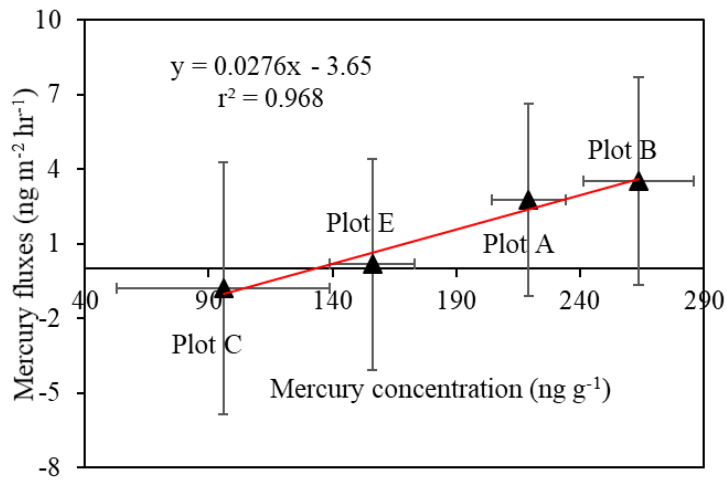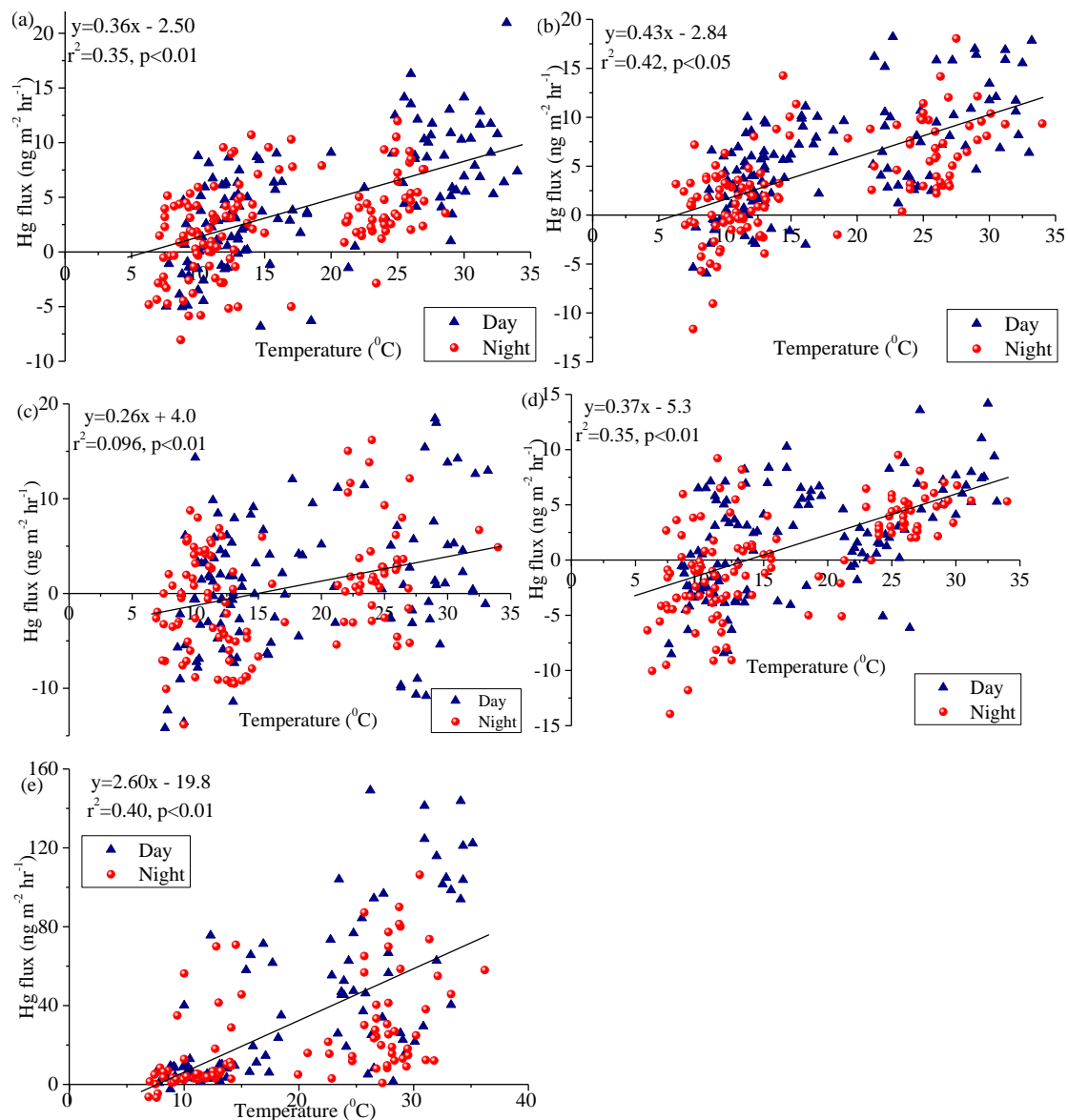
Fig. S5. Correlation between the soil Hg concentrations ($S_c \pm SD$) and soil-air Hg flux ($F \pm SD$) under the forest canopy at the subtropical forest. Standard deviations of soil Hg concentrations were obtained from Hg concentrations over the four seasons (n=12). Because fluxes are often controlled by solar radiation for bare soils, the correlation analysis above does not include data from the open field (plot E).
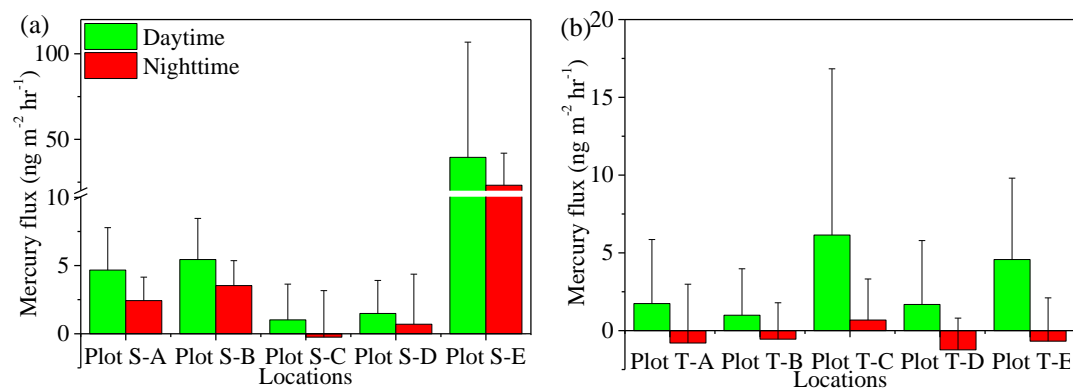
Fig. S6. Soil-air TGM fluxes during the daytime and nighttime at Masson pine forests (Plot A) and (Plot B), wetland (Plot C), evergreen broad-leaved forest (Plot D) and open field (Plot E) at the subtropical forest (a), and at Chinese pine forest (Plot A), larch forest (Plot B), wetland (Plot C), mixed broad-leaved forest (Plot D) and open field (Plot E) at the temperate forest (b).

Fig. S7. Correlations between soil temperature and air-surface Hg fluxes measured during daytime and night at the Masson pine forests (a) and (b), wetland (c), evergreen broad-leaved forest (d) and open field (e) in the subtropical forest.
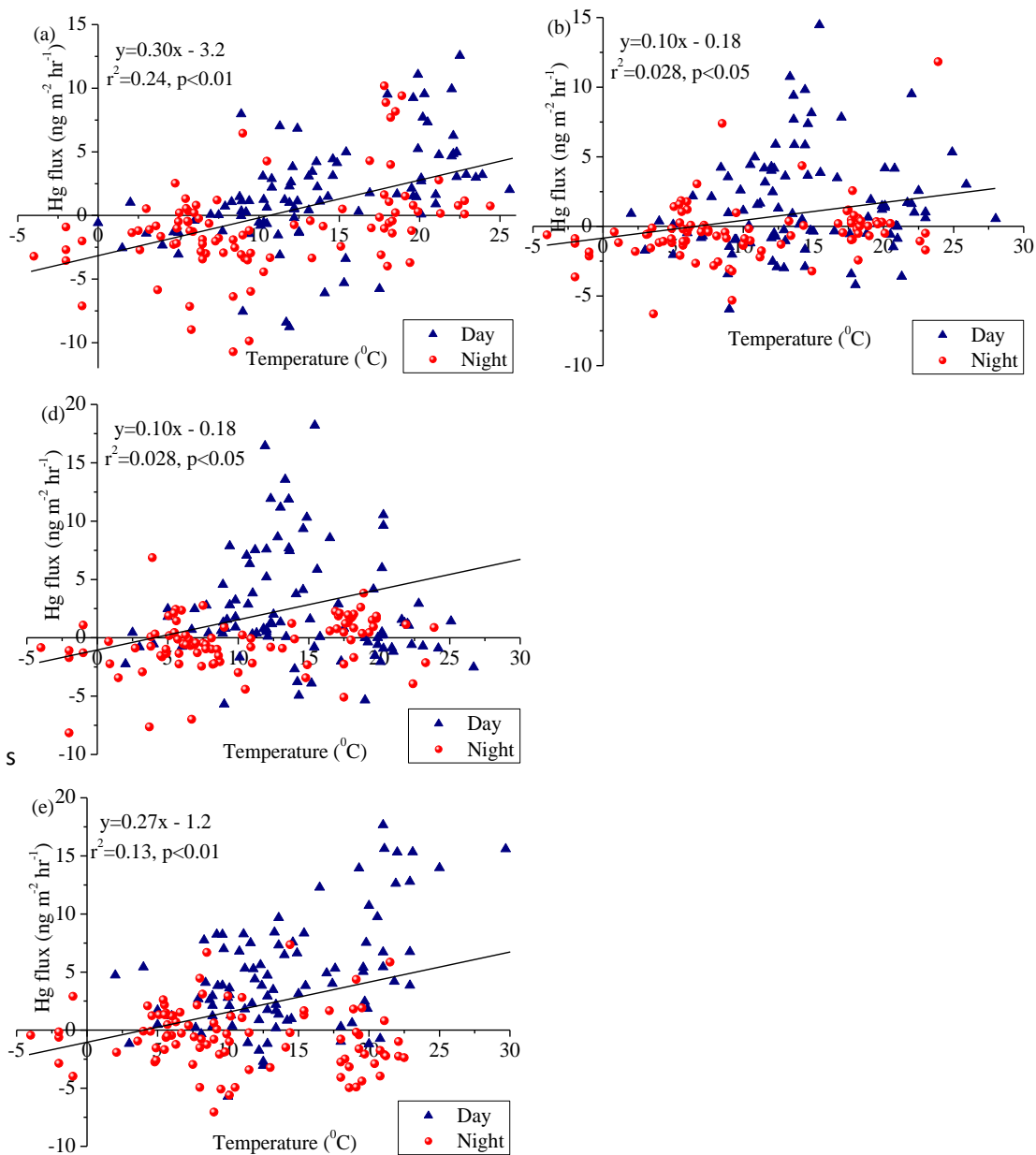
1230

1231   s

1232

Fig. S8. Correlations between soil temperature and air-surface Hg fluxes measured during daytime
and night at the Chinese pine forest (a), larch forest (b), wetland (c), mixed broad-leaved forest (d)
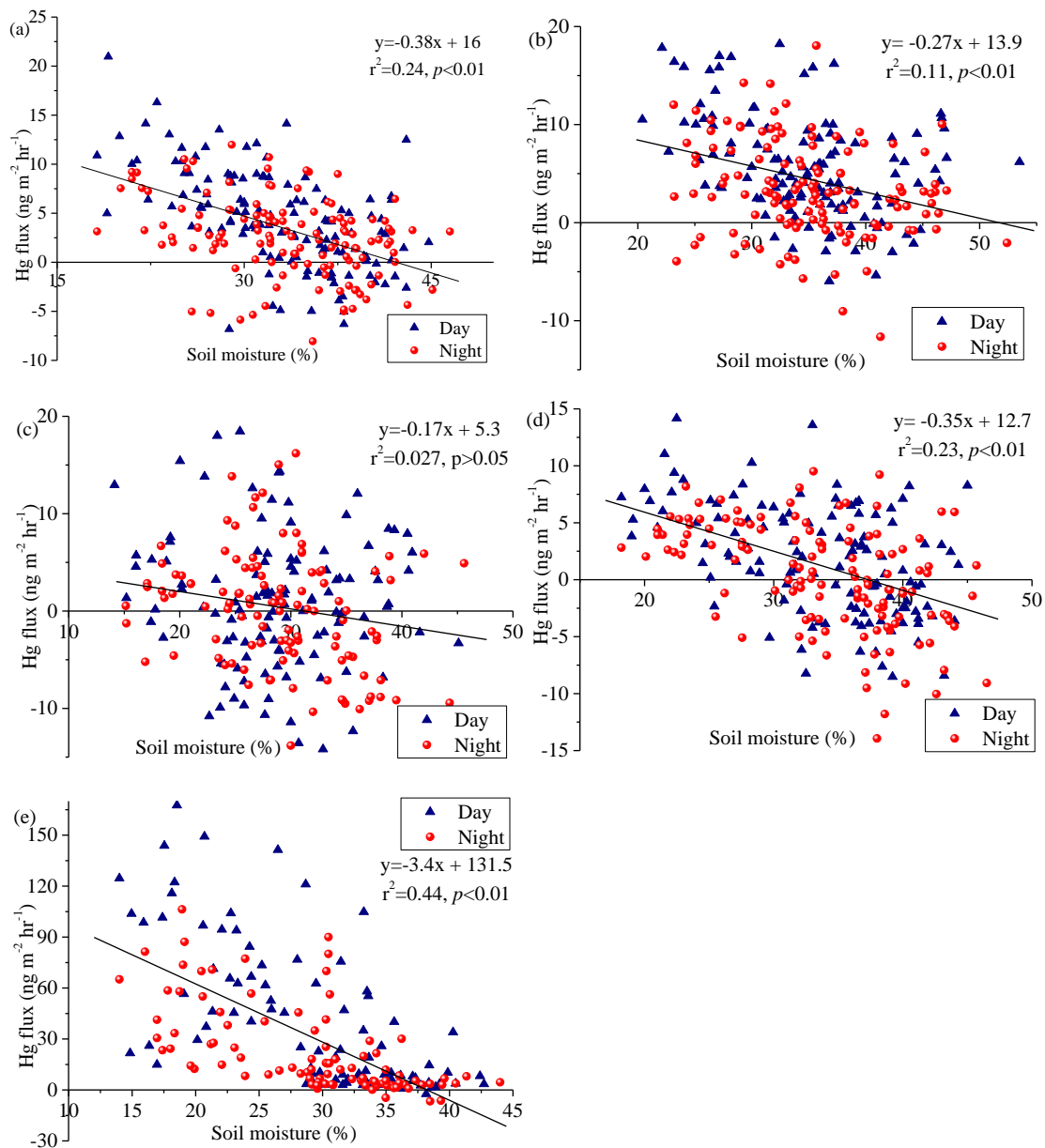and open field (e) at the temperate forest.

1237

1238

1239

Fig. S9. Correlations between soil moisture and air-surface Hg fluxes measured during daytime and
night at the Chinese pine forest (a), larch forest (b), wetland (c), mixed broad-leaved forest (d) and
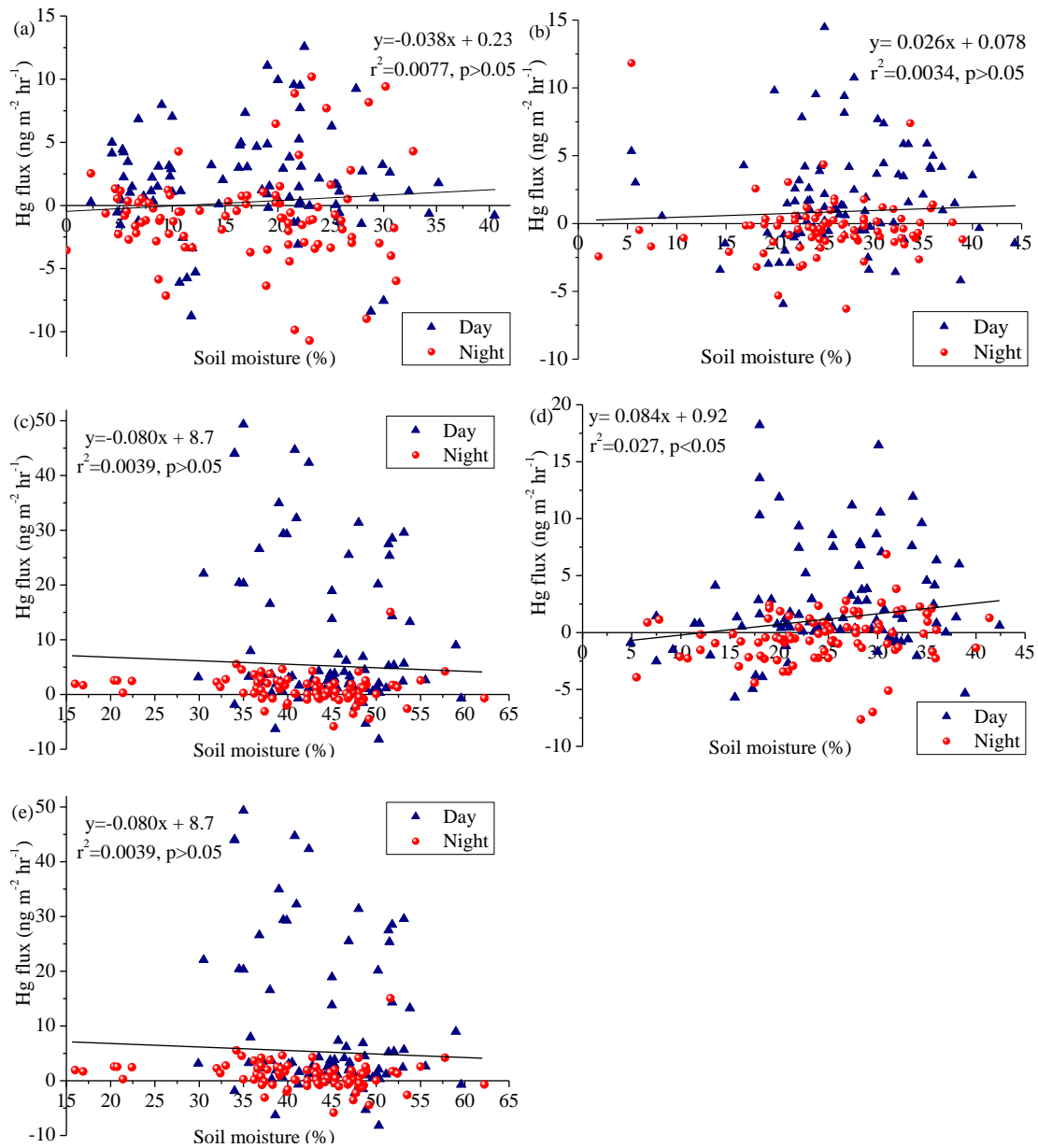open field (e) at the subtropical forest.

Fig. S10. Correlations between soil moisture and air-surface Hg fluxes measured during daytime and night at the Chinese pine forest (a), larch forest (b), wetland (c), mixed broad-leaved forest (d) and open field (e) at the temperate forest.
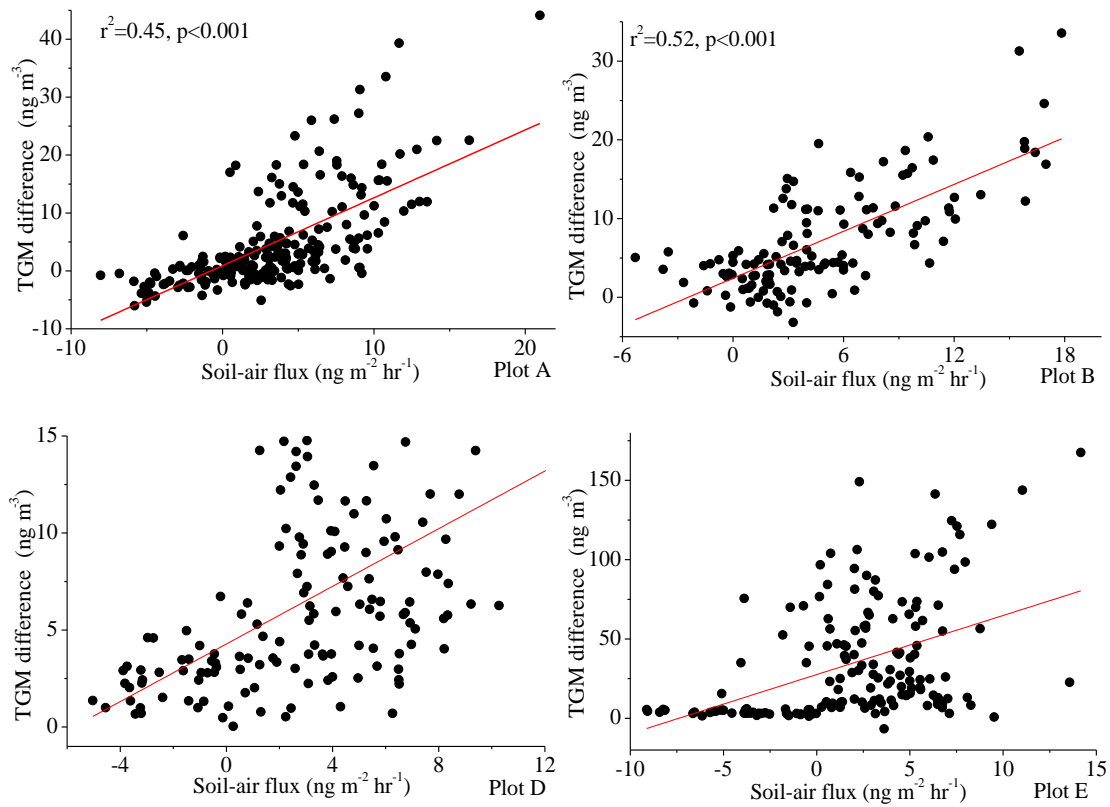
1251

1252

Fig. S11. Correlations between the gradient of Hg(0) concentrations between surface soil pore (at 3
cm) and atmospheric values and soil-air Hg(0) flux at four plots at the subtropical forest.
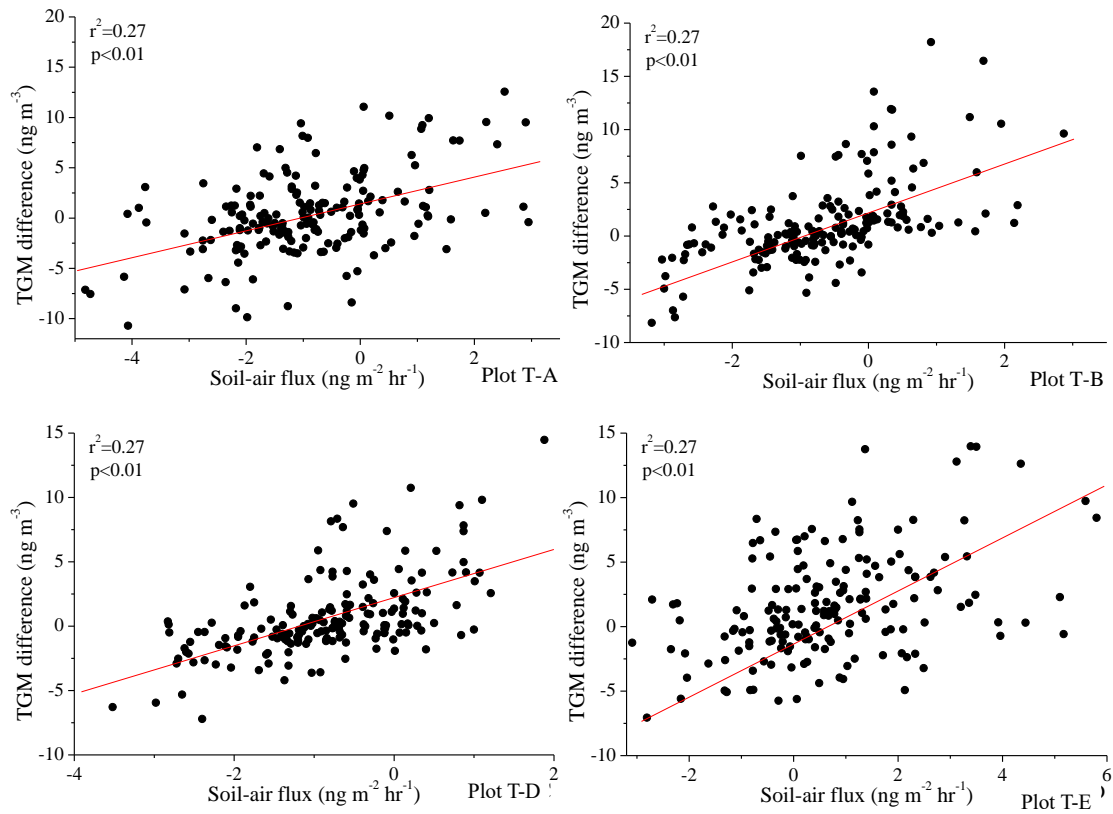
1255

1256

1257

Fig. S12. Correlations between the gradient of Hg(0) concentrations between surface soil pore (at 3
cm) and atmospheric values and soil-air Hg(0) flux at the four plots at the temperate forest.

1258

1259

1260

References:

Zhou, H., Ma, K., and Fu, B.: Analysis of the impacts of human activities on landscape patterns in dangling mountain area of Beijing, J Nat Resour, 14, 117-122, 1999.

Zhou, J., Feng, X., Liu, H., Zhang, H., Fu, X., Bao, Z., Wang, X., and Zhang, Y.: Examination of total mercury inputs by precipitation and litterfall in a remote upland forest of Southwestern China, Atmospheric Environment, 81, 364-372, 10.1016/j.atmosenv.2013.09.010, 2013.

Zhou, J., Wang, Z., Zhang, X., and Chen, J.: Distribution and elevated soil pools of mercury in an acidic subtropical forest of southwestern China, Environmental Pollution, 202, 187-195, 10.1016/j.envpol.2015.03.021, 2015.

Zhou, J., Wang, Z., Sun, T., Zhang, H., and Zhang, X.: Mercury in terrestrial forested systems with highly elevated mercury deposition in southwestern China: The risk to insects and potential release from wildfires, Environmental Pollution, 212, 188-196, 10.1016/j.envpol.2016.01.003, 2016.

Zhou, J., Wang, Z., Zhang, X., and Gao, Y.: Mercury concentrations and pools in four adjacent coniferous and deciduous upland forests in Beijing, China, Journal of Geophysical Research: Biogeosciences, 122, 1260-1274, 2017.

Zhu, J., Mulder, J., Solheimslid, S. O., and Dörsch, P.: Functional traits of denitrification in a subtropical forest catchment in China with high atmogenic N deposition, Soil Biology and Biochemistry, 57, 577-586, https://doi.org/10.1016/j.soilbio.2012.09.017, 2013.